iScience

CellPress
OPEN ACCESS

Article

Bioelectrochemically enhanced degradation of bisphenol S: mechanistic insights from stable isotope-assisted investigations

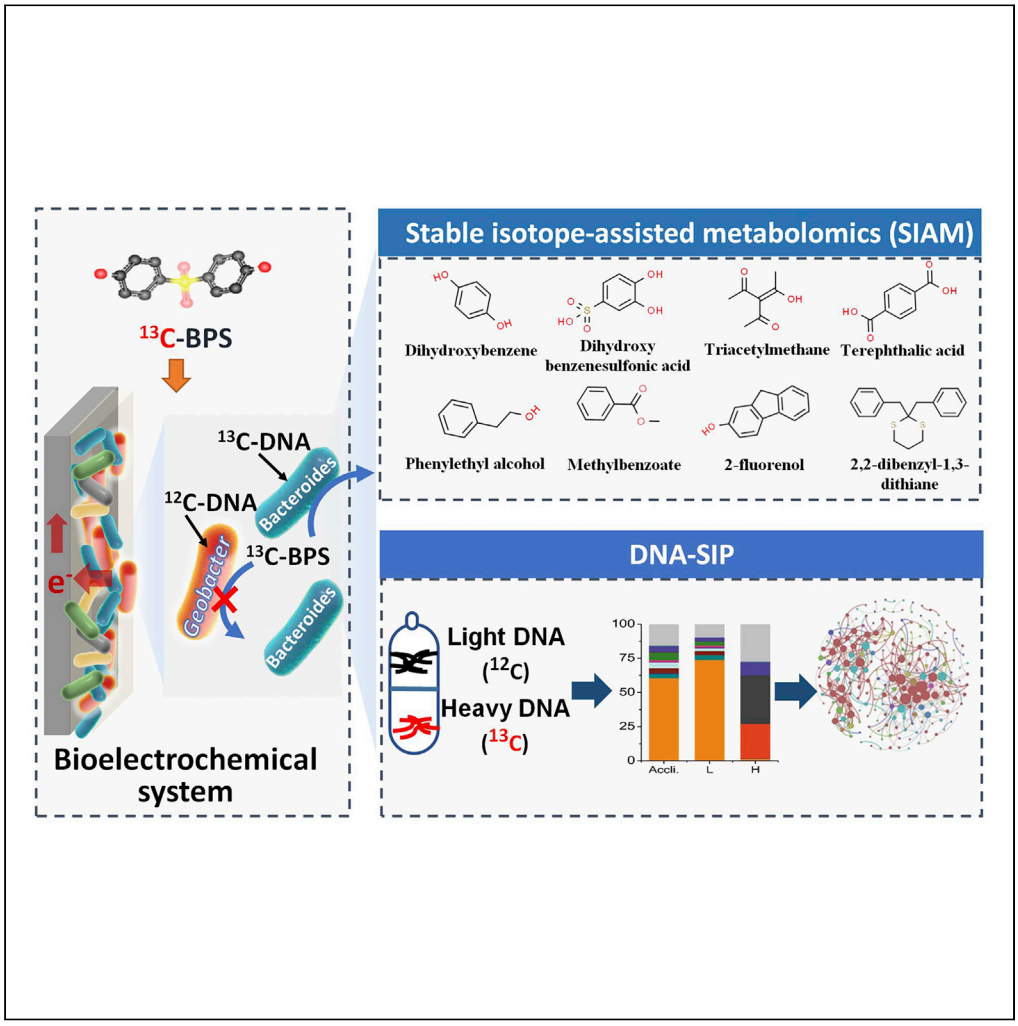

Rui Hou, Lin Gan, Fengyi Guan, Yi Wang, Jibing Li, Shungui Zhou, Yong Yuan

yuanyong@soil.gd.cn

HIGHLIGHTS

BPS can be effectively degraded by the electroactive biofilms in BES

DNA-SIP showed *Bacteroides* and *Cetobacterium* were the dominant BPS assimilators

SIAM highlighted hydrolysis and oxidation as initial degradation pathways for BPS

The enhanced degradation is attributed to interactions between EAM and degradators

Hou et al., iScience *24*, 102014
January 22, 2021
https://doi.org/10.1016/j.isci.2020.102014

iScience

CellPress
OPEN ACCESS

Article

Bioelectrochemically enhanced degradation of bisphenol S: mechanistic insights from stable isotope-assisted investigations

Rui Hou,[1] Lin Gan,[1] Fengyi Guan,[1] Yi Wang,[1] Jibing Li,[2] Shungui Zhou,[3] and Yong Yuan[1,4,*]

SUMMARY

Electroactive microbes is the driving force for the bioelectrochemical degradation of organic pollutants, but the underlying microbial interactions between electrogenesis and pollutant degradation have not been clearly identified. Here, we combined stable isotope-assisted metabolomics (SIAM) and ^{13}C-DNA stable isotope probing (DNA-SIP) to investigate bisphenol S (BPS) enhanced degradation by electroactive mixed-culture biofilms (EABs). Using SIAM, six ^{13}C fully labeled transformation products were detected originating via hydrolysis, oxidation, alkylation, or aromatic ring-cleavage reactions from ^{13}C-BPS, suggesting hydrolysis and oxidation as the initial and key degradation pathways for the electrochemical degradation process. The DNA-SIP results further displayed high ^{13}C-DNA accumulation in the genera *Bacteroides* and *Cetobacterium* from the EABs and indicated their ability in the assimilation of BPS or its metabolites. Collectively, network analysis showed that the collaboration between electroactive microbes and BPS assimilators played pivotal roles the improvement in bioelectrochemically enhanced BPS degradation.

INTRODUCTION

Bioelectrochemical system (BES) is a sustainable technology that can provide continuous electrons to enhance bioremediation efficiency through a combination of biological and electrochemical processes (Miran et al., 2018; Wang et al., 2016). BESs have been applied for in degradation of various recalcitrant pollutants, such as BTEX compounds (benzene, toluene, ethylbenzene, and xylenes) (Daghio et al., 2018), sulfa drugs (Miran et al., 2018; Wang et al., 2016), halogenated aromatic hydrocarbons (2-fluoroaniline, 2,4,6-trichlorophenol, and 2,4-dichlorophenol) (Cao et al., 2016; Xu et al., 2018; Zhang et al., 2014), and organophosphate esters (Hou et al., 2019). A mixed-culture BES exhibited the most promising stable electrochemical expression and degradation cooperation (Ng et al., 2017), and the electricity generated by electrochemically active biofilms (EABs) was deemed the central driving force for the biocatalysis of recalcitrant compounds in the BES (Hou et al., 2019). The degradation of organic pollutants is commonly accomplished by anodic oxidation by EABs, where the pollutant discharges electrons to oxidative metabolites (Hasany et al., 2016; Song et al., 2016). Therefore, comprehensive investigation of the microbial community and pollutant transformation in BES is crucial and will lead to a better understanding of bioelectrochemical reaction mechanisms and assessment of treatment efficiency (Yan et al., 2019).

Considering that most electroactive microbes (EAMs) in EABs can only use restricted substrates as electron donors, such as acetate and glucose (Chae et al., 2009; Fernando et al., 2019; Kiely et al., 2011; Logan et al., 2019), several studies recognized that unique non-EAMs in EABs were responsible for metabolizing organic pollutants (Capellades et al., 2016; Yan et al., 2019). The degradation process for organic pollutants can be divided into the decomposition of complex compounds by non-EAMs and the subsequent utilization of simple products by EAMs (Cao et al., 2020). To reveal the actual microbial characteristics during the electrochemical degradation of organic pollutants in BES, high-throughput sequencing and even metagenomic approaches have been used to scan the pollution-associated microbiome in EABs. The existence of target organic pollutants can alter the microbial community on the anode surface of the BES, where some microbial communities with unique pollutant degradation capacities were enriched on acclimatized EABs (Hou et al., 2019; Lu et al., 2014; Pham et al., 2009; Yan et al., 2017). It was suggested that the coexistence and the potential synergy between EMs and multiple organic-degrading microbes may be the underlying

[1]Guangzhou Key Laboratory Environmental Catalysis and Pollution Control, Guangdong Key Laboratory of Environmental Catalysis and Health Risk Control, School of Environmental Science and Engineering, Institute of Environmental Health and Pollution Control, Guangdong University of Technology, Guangzhou 510006, China

[2]State Key Laboratory of Organic Geochemistry, Guangzhou Institute of Geochemistry, Chinese Academy of Sciences, Guangzhou 510640, China

[3]Fujian Provincial Key Laboratory of Soil Environmental Health and Regulation, School of Resources and Environment, Fujian Agriculture and Forestry, Fuzhou 350000, China

[4]Lead contact

*Correspondence: yuanyong@soil.gd.cn

https://doi.org/10.1016/j.isci.2020.102014

mechanisms for the enhanced degradation of biorefractory compounds in BES (Hou et al., 2019). However, the contribution of non-EAMs to pollutant degradation and the possible interaction mechanisms between EAMs and non-EAMs during pollutant degradation are still unknown.

The degradation pathways for several biorefractory compounds in mixed-culture EABs have been previously demonstrated via target screening methods using high-resolution mass spectrometry. For example, the degradation pathway of sulfamethoxazole in a BES was determined to include the cracking of S–N bonds, N–O bonds, and carbon–carbon double bonds (Wang et al., 2016); and oxidized furan derivatives, open-ring products, and dimers were generated from the bioelectrochemical transformation of furanic and phenolic compounds via exoelectrogenesis (Zeng et al., 2015). However, targeted screening methods for metabolite identification require predetermined or suspected metabolic pathways, which may overlook potential novel pathways, reaction priority, and sequences (Creek et al., 2012). In the targeted method, secondary analytical approaches are also needed for confident identification, where the purchase, synthesis, or isolation of pure authentic metabolite standards is required (Creek 2013). The degradation mechanisms for xenobiotic pollutants are quite complicated in BESs with different operation modes, and the detected products may not derive from classical pathways, even in well-defined bioelectrochemical processes (Yan et al., 2019). Therefore, there is still a limitation on the ability to determine pollutant degradation processes and mechanisms in BESs with traditional target screening methods.

In recent years, pathway identification and mechanism elucidation in bioremediation processes have progressed, aided by advancements in stable isotope probing (SIP) techniques, such as DNA-SIP and stable isotope-assisted metabolomics (SIAM). DNA-SIP allows the identities of microorganisms in environmental samples to be linked with their activities and functions using particular growth substrates that are highly enriched in a stable isotope (e.g., ^{13}C or ^{15}N) (Bernard et al., 2007; Dumont and Murrell 2005; Zhan et al., 2018). This technique has been used to identify the functional microbes in the biodegradation of a large number of pollutants, including pharmaceuticals and personal care products (Badia-Fabregat et al., 2014), phenanthrene (Jones et al., 2011; Li et al., 2017b), bisphenol A (Sathyamoorthy et al., 2018), triclosan (Lee et al., 2014), and nonylphenol (Zemb et al., 2012). For bioelectrochemical process, DNA-SIP has also been used to identify the predominant roles of *Geobacter sulfurreducens* and *Hydrogenophaga* in acetate consumption and current generation in microbial fuel cells (Kimura and Okabe 2013). However, few studies have applied DNA-SIP to investigate the microbial mechanisms of pollutant degradation by EABs. In addition, SIAM can provide the identification of stable isotopes labeled metabolites on a global scale through comparing to their nonlabeled pendants according to appropriate experimental protocols (e.g., X^{13}CMS, geoRge, and MetExtract II) (Baran et al., 2010; Bueschl et al., 2017; Capellades et al., 2016; Creek et al., 2012). Recently, SIAM has been applied to quantitatively unveil a variety of biological processes, such as carbon and nitrogen fixation by *Synechococcus sp.* (Baran et al., 2010), the intracellular metabolic fluxes of *G. sulfurreducens* under different electron donors (Yang et al., 2010), and the biotransformation of polycyclic aromatic hydrocarbons in soil (Tian et al., 2018). Inspired by these studies, the combination of these stable isotopic tracing techniques is expected to offer an opportunity to elucidate not only the global pollutant transformation pathways but also key microbial interplay mechanisms between EAMs and non-EAMs for pollutant degradation in BESs.

Bisphenol S (4-hydroxyphenyl sulfone; BPS) is one of the major substitutes for the replacement of bisphenol A (BPA) in various applications with endocrine-disrupting effects of concern (Ruth and Louise 2015). BPS exhibits similar structures and environmental behaviors to other bisphenol analogues including BPA (Chen et al., 2016), and similar removal effect of BPS is expected for BES (Li et al., 2019). However, to the best of our knowledge, there is a limited report on the removal strategies of BPS in the bioelectrochemical approach and the unique microbial cooperation mechanisms in EAMs during degradation of this kind of pollutants. In this study, we expand the application of SIP to elucidate the biodegradation mechanisms of BPS by acclimated EABs in a three-electrode BES, combining the technologies of DNA-SIP and SIAM. Our objectives were (1) to investigate the relationship between electricity generation characteristics and the removal kinetics of BPS in acclimated EABs; (2) to apply SIAM to identify the global biodegradation pathways for BPS; and (3) to utilize DNA-SIP to characterize the contributions of EAMs and non-EAMs in biofilms and BES suspensions to BPS degradation. These results might provide novel information on microbial behavior in the bioelectrochemical remediation of biorefractory compounds and promote the better exploitation of appropriate BES strategies.

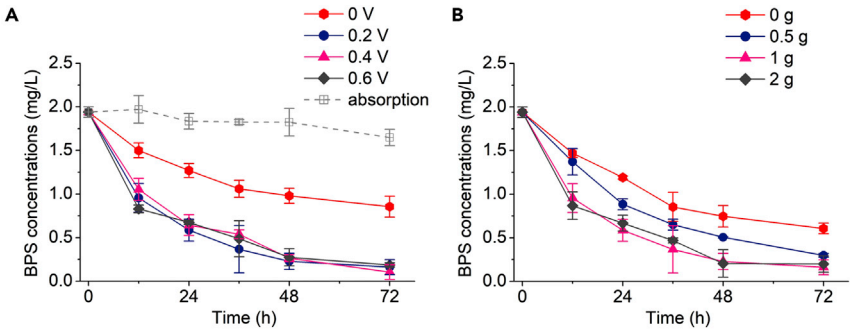

Figure 1. BPS degradation by the acclimatized biofilm in BESs

(A) degradation curves under different external voltages.

(B) degradation curves under different sodium acetate concentrations. Other test conditions: BPS 2 mg/L, ambient temperature (28 ± 2°C), pH = 7.0. Data are represented as mean ± SEM.

RESULTS

Bioelectrochemical degradation of BPS in the BESs

Figure S1 shows the changes in the BPS biodegradation ratio in the BES reactors during 9 cycles of acclimation, at the initial administrated concentration of 2 mg/L. BPS was rather difficult to remove over the 48 hr after it was initially added to the reactors. After acclimation to BPS, it was found that the changes in BPS concentration in the BESs were rather obvious, where approximately 78.2% of the BPS was removed after 48 h of operation. On the other hand, the reactor current density severely declined and then gradually increased to 4.0 mA/cm^2, which indicated that the metabolic activity of EAMs inhibited by BPS was recovered and that the reactor microbes became highly efficient at BPS removal after 9 cycles of operation.

Three different modes of BES reactors were tested for comparison, including a closed-circuit mode, an open-circuit mode, and an abiotic control. Figure 1A shows the degradation kinetics of 2 mg/L BPS during 72 h of incubation for the BES groups. Significant changes in BPS concentration were observed in all closed-circuit groups, with the 72 h degradation ratios for BPS calculated as 55.9%, 91.7%, 94.6%, and 90.4% under anode potentials of 0, 0.2, 0.4, and 0.6 V, respectively. However, only approximately 15.1% and 24.8% of BPS was removed in the abiotic control and open-circuit groups after 72 h of operation, respectively. These results indicated that the physical adsorption of BPS by the BES anode was slight and that the existence of an electric field in the BES reactors could increase the removal of BPS. In addition, the calculated pseudo-first order rate constants (k) for BPS at an anode potential of 0 V were significantly lower than those at anode potentials of 0.2, 0.4 and 0.6 V (Table S1; $p < 0.05$), but no significance was found among the degradation rate constants of BES reactors at anode potentials of 0.2, 0.4 and 0.6 V ($p > 0.05$). This phenomenon is in agreement with previous studies in which EAMs at 0.2 V exhibited higher catalytic activity than those at other potentials ranging from −0.1 V to +0.6 V (Li et al., 2017a).

To ascertain the role of the acclimatized EAMs in BPS removal in the BESs, the degradation kinetics of BPS were evaluated under various sodium acetate concentrations (Figure 1B). The BES without sodium acetate showed a BPS removal of only 68.7%, and this removal increased significantly to 84.6% when 0.5 g/L sodium acetate was added at the beginning of incubation into the BES as cosubstrate. BPS degradation in the BES with 2 g/L sodium acetate showed the highest rate constants (Table S1). The results were in accord with previous studies on the enhanced degradation of aromatic compounds in BESs obtained by supplementing carbon cosubstrates (Fan et al., 2017; Luo et al., 2009). We also found elevated electricity generation with increasing sodium acetate concentrations in the BESs (Figure S2). Therefore, the acceleration in the removal of BPS in the BESs can be linked to the presence of the anode in providing an electron transfer pathway to enhance the metabolic rate of bacteria using acetate as an electron acceptor (Miran et al., 2018). The permeability of the cell membrane, increasing the absorbance of extracellular substances, and altering the microbial metabolism of EAMs caused by an electric field might also be the possible reason for the enhancement of BPS degradation in BESs (Hasany et al., 2016; Saratale et al., 2017; Yan et al., 2019).

Table 1. Detected metabolites of BPS from the processed feature groups obtained by MetExtract

Features	RT	Ionization	m/z ^{12}C	m/z ^{13}C	Xn	Formula	ΔMass (ppm)	Tentative idenetification	Confidence level[a]	CSID	Intensities (peak area)
Fg1	2.00	+	143.06884	150.09600	7	$C_7H_{10}O_3$	17.5	Triacetylmethane	2	63143	14176.89
Fg2	2.08	+	111.04402	117.04654	6	$C_6H_6O_2$	35.0	Dihydroxybenzene	2	13837760	25479.99
Fg3	2.19	–	165.02900	173.05578	8	$C_8H_6O_4$	34.8	Terephthalic acid	2	7208	18748.60
Fg4	2.21	+	123.07332	131.09021	8	$C_8H_{10}O$	−26.0	Phenylethyl alcohol	3	5830	16239.42
Fg5	2.28	–	188.99243	194.99495	6	$C_6H_6O_5S$	11.6	Dihydroxy benzenesulfonic acid	3	164229	45024.94
Fg6	2.95	+	137.05917	145.08602	8	$C_8H_8O_2$	24.7	Methylbenzoate	3	6883	13064.11
Fg7	14.98	–	249.02292	261.06318	12	$C_{12}H_{10}O_4S$	18.7	BPS	1	6374	935016.75
Fg8	15.23	+	183.08249	195.12288	12	$C_{13}H_{10}O$	32.6	2-fluorene	3	68072	10786.83
Fg9	17.29	+	301.10167	313.14183	12	$C_{18}H_{20}S_2$	−7.7	2,2-dibenzyl-1,3-dithiane	2	530757	17060.69

[a]Confidence levels for metabolite identification were assigned according to the criteria established by Schymanski et al. Level 2: tentative candidates (compounds identified by molecular formula and substructures), based on accurate mass, MS/MS pattern, and database search. Level 3: unequivocal molecular formula based on accurate mass, but no other supporting data.

Metabolites and novel pathway of BPS biodegradation as revealed by SIAM

To unequivocally demonstrate the degradation mechanisms of BPS in BESs, we employed an untargeted SIAM study, wherein a 1:1 ratio of ^{12}C- and $^{13}C_{12}$-BPS was used as substrate with sodium acetate. A total of 13 feature groups were detected in full-scan chromatograms of samples using MetExtract (Figures 2 and S3–S5). The nonlabeled and the corresponding isotopically labeled metabolites were matched to the ion pairs, and the different feature pairs originating from the same transformed products (TPs) were convoluted into one feature group. All the corresponding feature groups for the detected TPs showed divisible mass differences from 2 to 12 times the mass of a neutron (1.0033 Da), indicating the presence of 2–12 isotopic carbon atoms in the features (Table 1). For all the detected TPs, their tentative structures were assigned based on the exact mass, MS/MS fragmentation patterns and deduced number of labeled carbons, which were processed with the Compound Discovery platform and searched in the Chemspider database (Table 1, Figure S3 and S4). The identity of BPS (Fg 7) was confirmed by measurements of the ^{12}C-BPS standard (Level 1 certainty, Schymanski et al. (2014)). Among these detected TPs, 7 formulas (Fg 1, 2, 3, 7, and 9) were qualified with both the exact mass and MS/MS fragmentation patterns (Level 2 certainty with diagnostic evidence). However, the other 5 TPs (Fg 4, 5, 6, and 8) could only be tentatively identified with MS data, but the MS/MS data were insufficient to confirm their structures (Level 3 certainty) (Figure S6).

Accordingly, except for BPS, three major groups of TPs were detected in the BES suspension, and the specific degradation pathway of BPS was tentatively proposed as shown in Figure 3. In the first group, we detected two formulas (Fg 2, dihydroxybenzene, $C_6H_6O_2$; and Fg 5, dihydroxybenzene sulfonic acid, $C_6H_6O_5S$) originating from the hydroxylated hydrolysis products, which all contained 6 labeled carboxyl groups. The two TPs from the first and second groups (i.e., Fg 2 and Fg 5) were also exhibited relatively higher peak intensities than those of other detected TPs. Previous studies on advanced oxidative degradation of BPS also reported the formation of these two TPs (Kovačič et al., 2019; Luo et al., 2019). This result suggested the hydrolysis and oxidation processes were the initial and key transformation pathways for bioelectrochemical degradation of BPS. The second groups of the features (Fg 1, 3, 4, and 6) were formed through the pathways of alkyl substitution, rearrangement and oxidation from the hydrolysis TPs. All of the carbon skeletons in each of these compounds were labeled with ^{13}C. Fg 1 and Fg 3 were identified using their MS/MS fragmentation patterns as triacetyl methane and terephthalic acid, respectively, and the other accumulated TPs (Fg 4 and Fg 6) were hypothesized to be phenylethyl alcohol and methylbenzoate, respectively, according to their exact mass. Therefore, we propose that further oxidation, alkylation, and aromatic ring-cleavage reactions occurred as the next degradation pathways for BPS.

For the third group of TPs, the two features both had twelve labeled carbons in their ^{13}C paired ions, which means that unlabeled carbons occurred in their structure. The two TPs (Fg 8 and Fg 9) were assigned

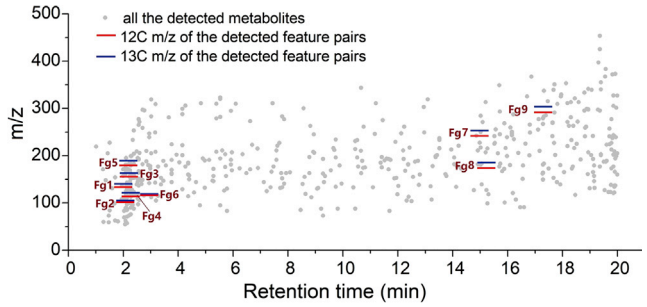

Figure 2. Comparison visualization of the extracted native (^{12}C; red line) and labeled (^{13}C; blue line) feature groups

The metabolites shown in gray are unmatched ions.

to 2-fluorenol and 2,2-dibenzyl-1,3-dithiane, respectively. It was indicated that carbon-carbon (C-C), carbon-oxygen (C-O) or multivalent couplings occurred in the formation of these resultant dimers from hydrolysis products of BPS by constant transfer of electrons (Wang et al., 2017; Zeng et al., 2015). The results indicated that ^{13}C-labeled byproducts (i.e., CH_3OH, CH_3CHO, HCHO, C_2H_5OH, etc.) from the first and second degradation pathways can be reprocessed by EAMs to reconstitute low-isotopic-ratio products.

The formation of the low-isotopic-ratio products (i.e., the third group) indicated that monomeric product coupling and carboxyl coupling as the further BPS degradation pathways, which reflects the complexity of the degradation process for BPS in BES. For the TPs from the third degradation pathways, considering that no previous research has described these complex degradation processes in BES, the structural formula and possible compounds can only be roughly inferred according to the exact mass number of ions. The best explanation for most of these detected TPs is anabolic and catabolic processes in microbial metabolism. The oxidative products of BPS from the first and second groups had a variety of hydroxyl, aldehyde, ketone, sulfate or carboxyl groups, which might contribute to cross-linking reactions with various ^{12}C organic substrates. A previous study observed that several hydroxylated PAH metabolites were able to undergo coupling reactions with compounds in natural organic matter through ether, C-C, or multivalent bonds during microbial degradation (Kästner et al., 1999). In addition, coupling reactions can be enhanced by chemoautotrophic EAMs when taking up electrons from the electrode to transform substrates into products containing more carbon (Pellis et al., 2018; Rabaey and Rozendal 2010; Srikanth et al., 2018). Accordingly, it is possible for EAMs to utilize directly degraded metabolites to form low-isotopic-ratio TPs; the environmental safety of these compounds is also currently unknown and needs to be further investigated.

Identification of microorganisms assimilating ^{13}C-BPS in BES

After ultracentrifugation of the DNA extracted from the ^{13}C-BPS assimilated biofilm and BES suspension, the "light" and "heavy" fractions were selected according to the total DNA concentrations across the isotopically fractionated gradients (Figure S7). The DNA concentration curves for gradient fractions from the ^{12}C-BPS assimilated biofilm and BES suspension both indicated a single peak in the mass range of 1.72–1.74 g/mL. A similar trend was also found in the DNA curve for the ^{13}C-BPS assimilated suspension, whereas in the ^{13}C-BPS assimilated biofilm, a second higher peak for DNA concentration was present at a buoyant density of 1.75–1.77 g/mL. This result implies that some microbes that assimilated ^{13}C atoms derived from ^{13}C-BPS were successfully isolated by ultracentrifugation, which made their appearance in the "heavy" DNA fraction.

Accordingly, the "light" (^{12}C-L and ^{13}C-L) and "heavy" (^{12}C-H and ^{13}C-H) fractions of 16S rRNA were selected to be phylogenetically characterized by high-throughput Illumina sequencing, along with the noncentrifuged biofilm and suspension samples from the initial (Ini.) and acclimated (Accli.) BES (Figure 4A). *Proteobacteria* were the preponderant phylum in the noncentrifuged biofilm and suspension, accounting for greater than 47.3% of bacterial reads, and the genus *Geobacter* comprised between 12.7% and 60.4% of the bacterial reads in these biofilm samples (Figures 4A and S8). For the ^{13}C-BPS SIP experiment, significant shifts in community composition were observed between the "heavy" and "light" DNA fractions of the

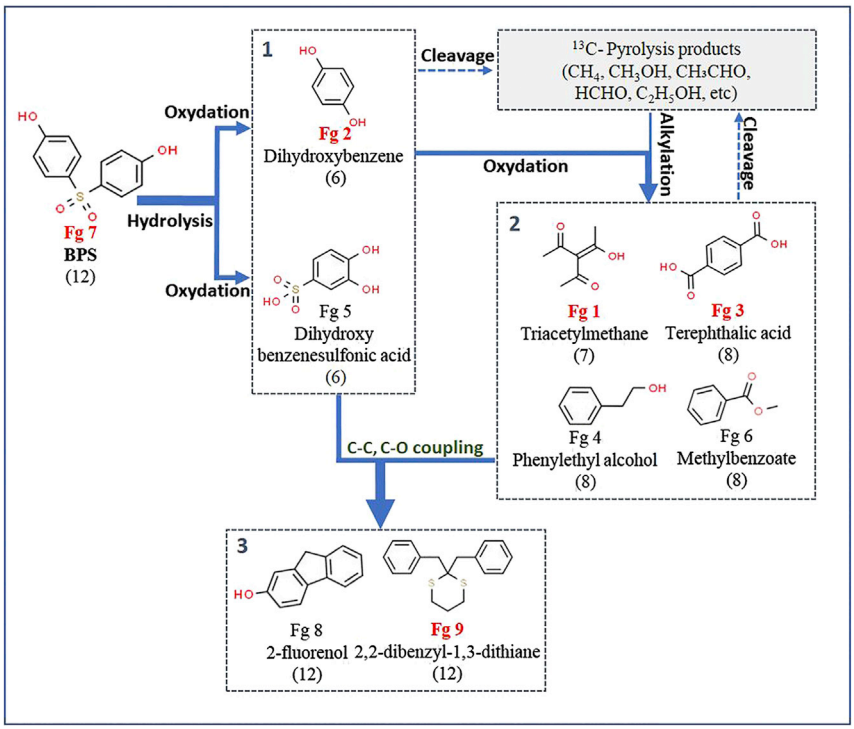

Figure 3. Proposed degradation pathway for BPS based on detected metabolites

Note that substituent positions are either inferred from known mass spectra or hypothesized. Transformation products (TPs) that have been validated by fragment mass spectrometry are labeled in red. The number of ^{13}C for each TP is indicated in brackets after its name. Pathways with solid arrows are predicted based on identified labeled metabolites in the current study and literature, and dotted arrows denote unknown pathways. Bold arrows represent higher flux and thin arrows represent stable isotope flux.

biofilm ($p < 0.05$). The relative abundances of *Bacteroides* and *Cetobacterium* in the "^{13}C-H" pooled samples were significantly higher than those measured in the "^{13}C-L" and "^{12}C-H" samples collected for SIP experiments or the noncentrifuged biofilm. However, there was no significant difference in the community composition of "^{13}C-L" and "^{13}C-H" from the BES suspension.

In addition, we assessed the relative abundances of the important microbes in each fraction from the biofilm and suspension of the SIP experiment (Figure 5). The results indicated that *Geobacter*, *Pseudomonas*, *Desulfovibrio,* and *Petrimonas* were not significantly enriched in the "heavy" BD fraction (>1.748 g/mL) in the ^{13}C-BPS biofilm and suspension samples compared with those in the ^{12}C-BPS samples. *Geobacter* can generate current using acetate as an electron donor (Yang et al., 2012); *Petrimonas* was also reported in previous studies to be a degradator of protein and carbohydrates in BESs (Kang et al., 2014); *Desulfovibrio* is associated with sulfate removal in BESs (Zheng et al., 2014); and *Pseudomonas* plays a key role in electron transfer media for nitrate and nitrite reduction (Zhang et al., 2014). Although these microbes are typical exoelectrogenic microbes in electrode biofilms (Lovley 2011), the present results suggested that these EAMs were not potential degradators of BPS in the BES.

Compared to the relative abundances of *Bacteroides* and *Cetobacterium* in the same fractions of the ^{12}C-BPS biofilm sample (0.82%, 0.45%, and 0.02%, respectively), the abundances in the heavy fractions from the ^{13}C-BPS biofilm sample were higher (35.4%, 10.0%, and 25.4%, respectively). Bacteria belonging to the genus *Bacteroides* were frequently detected in anodic biofilm (Call et al., 2009; Rismani-Yazdi et al., 2013; Zakaria and Dhar 2020), which also been suggested to have an important role in electricity generation in BES (Ha et al., 2012; Shehab et al., 2017). *Bacteroides* have also been previously identified as degradators of BPA or other aromatic hydrocarbon degradation (Comte et al., 2006; Yang et al., 2019). *Cetobacterium* most frequently occurs as gut microbes (Sheng et al., 2010) and sludge microbes (Song et al., 2015a; Tian

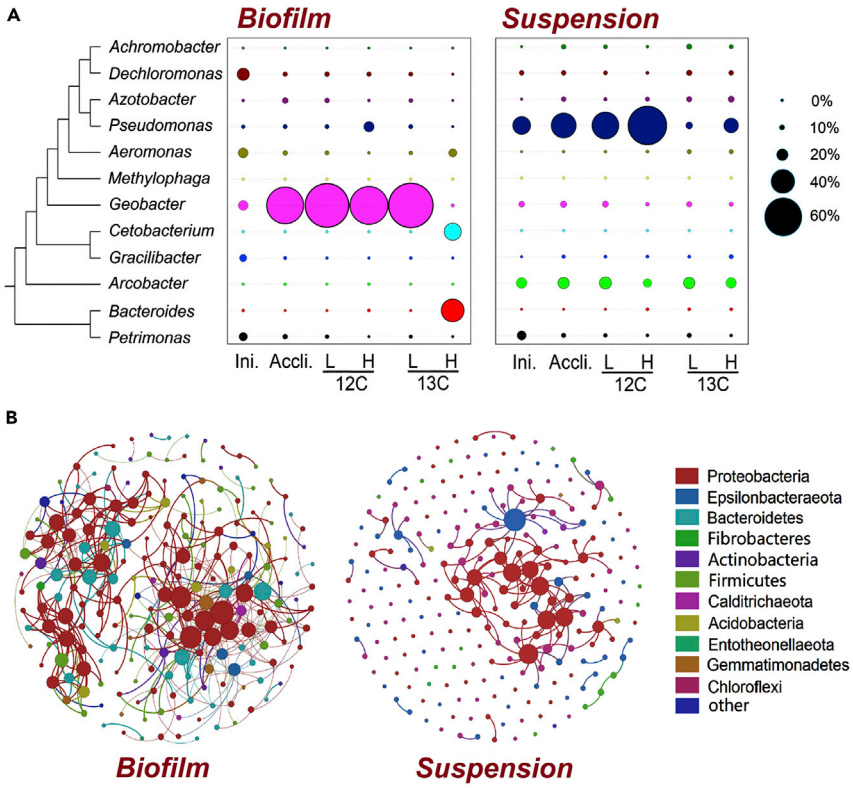

Figure 4. Phylogenetic tree and network associations in the BES biofilm and suspension

(A) Phylogenetic tree of bacterial 16S rRNA genes showing detected genera (left plot) and their relative abundance (right bubble plot) in (i) biomass collected from the light (L) and heavy (H) fractions from the ^{12}C and ^{13}C experiment and (ii) the initial (Ini.) and the acclimatized (Accli.) anode biofilm and suspension.

(B) the visualization of the bacterial network associations in the biofilm and suspension based on RMT analysis of OTU profiles.

et al., 2020), which were previously found to be involved in the consumption of alcohols (Bhute et al., 2020), fatty acids, and protein (Hao et al., 2017). Recent studies also found the existence of *Cetobacterium* in sludge and landfill sites (Song et al., 2015a; Tian et al., 2020) and their abilities in degradation of surfactants (Motteran et al. 2016, 2020), dye (Ji et al., 2020), and several aromatic compounds (Tian et al., 2020). The enhanced contributions of the electrode biofilms to BPS degradation in the BESs were likely derived from these microbes. Similar to the total DNA concentrations, *Bacteroides* and *Cetobacterium* were not enriched in the "heavy" BD fraction of the ^{13}C-BPS suspension, which confirmed the validity of our criteria for high-sensitivity SIP. Accordingly, these results suggested that the non-EAMs in EABs, rather than bacteria in the BES suspension, play key roles in the degradation of BPS, and *Bacteroides* and *Cetobacterium* may be preferentially involved in the degradation and assimilation of BPS and its metabolites.

Microbial interactions during bioelectrochemical degradation of BPS

After identification of the BPS-assimilating microbes, we constructed phylogenetic molecular ecological networks to determine the interspecies interaction between the typical EAMs and BPS-assimilating microbes in the BES biofilm and suspension (Figure 4B). As shown in Table S2, networks with 227 and 110 nodes were constructed from the biofilm and suspension samples, respectively, and the generated random networks showed significance of the network indices between the biofilm and suspension samples. Specifically, the values of density, average clustering coefficient, and transitivity in the suspension were statistically higher than those in the biofilm samples ($p < 0.01$), whereas the values of modularity, connectedness, and harmonic geodesic distance were significantly higher in the biofilm ($p < 0.01$). As expected, these phenomena suggest that the co-occurrence patterns of the bacterial communities in the biofilm and suspension were quite different, and the bacterial molecular ecological network in the biofilm was

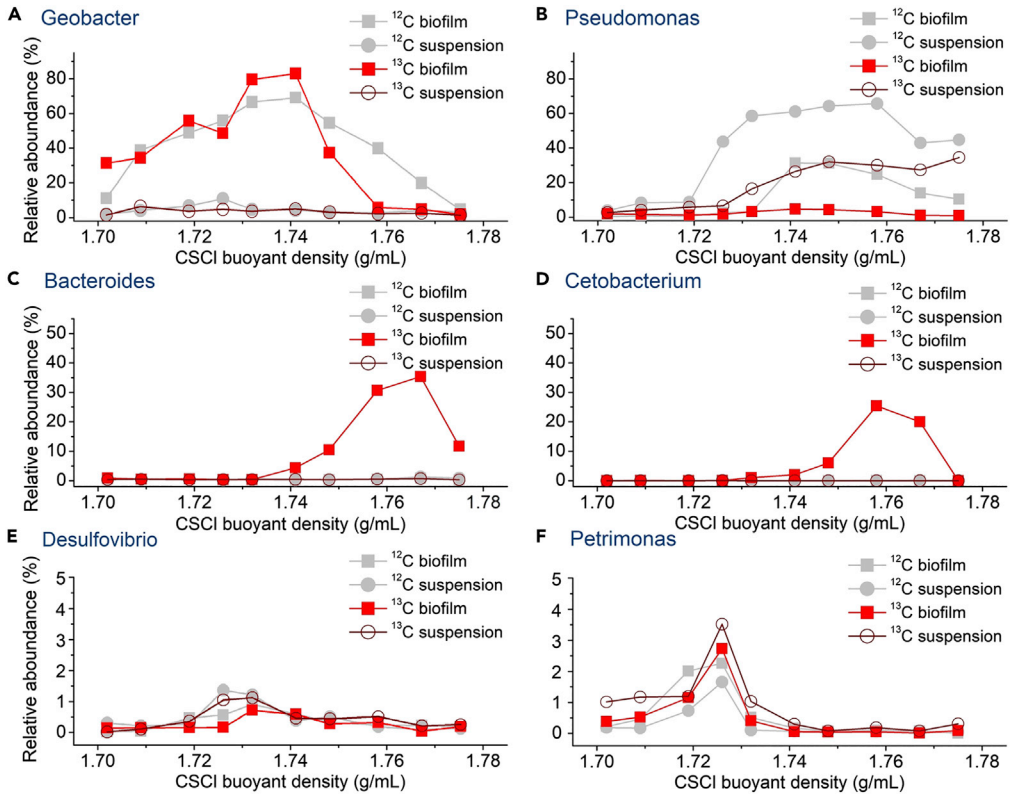

Figure 5. Relative abundance of representative bacterial genera across the entire buoyant density gradient of DNA fractions from the ^{12}C- and ^{13}C-BPS acclimatized biofilm and suspension

more complicated, intense, and centralized than that in the suspension. This community similarity was confirmed by the lower Shannon index for the biofilm than for the BES suspension (Table S3). The tighter microbial network interaction in the biofilms is also in accordance with the observation of higher ^{13}C accumulation in BES biofilms. Therefore, electron transfer between EABs and the electrode not only simultaneously enriched electrochemical bacteria and specific degradation bacteria but also enhanced their interaction as consortia.

According to the topographical roles of each node in the network (Figure S9), two nodes in the biofilm (OTU_2955, *Geobacter*; OTU_426, *Bacteroides*) were identified as keystone species in the bacterial network. Principal coordinates analysis (PCoA) using the weighted UniFrac approach was conducted to illustrate the difference of bacterial communities from BPS-acclimated biofilm and suspension (Figure S10A). Results from partial least squares discriminant analysis based cluster analysis (Figures S10B and S10C) well agreed with the PCoA analysis, where the bacterial genus such as *Geobacter* was identified to be the most dominant contributors to the separation based on their variable importance in projection values. These results suggested that electron transfer processes made EAMs (i.e., *Geobacter*) pivotal in the BPS-acclimated biofilm consortium, which resulted in the efficient and robust degradation of BPS via specific microbial metabolic interactions between EAMs and the (i.e., *Bacteroides* and *Cetobacterium*).

DISCUSSION

The present study first investigated the accelerated degradation of a novel bisphenol analog (i.e., BPS) in a BES using combined stable isotope-assisted approaches, which can provide a clear clue to the accelerated degradation mechanism of BPS. We identified that the genera *Bacteroides* and *Cetobacterium* accounted for the majority in assimilating BPS, and found that these assimilators were colonized in the biofilm but not suspended in the BES. *Cetobacterium* was not been reported as important components in the anodic biofilm from BES, but Bacteroides were identified as a fermentative bacterium which can produce the simple

organic acids from a wide range of substrates (i.e., glucose, acetate, cellulose, lactate, etc) to be utilized by EAMs (Jia et al., 2013; Wei et al., 2019). In a recent investigation of microbial communities from anodic biofilm via DNA-SIP (Song et al., 2015b), Bacteroides were not found to be involved in uptake ^{13}C-labeled sodium acetate, while *Geobacter, Rhodocyclaceae*, and *Pseudomonas* were the main contributors in the assimilation of acetate to conduct extracellular electron transfer in BES. Kimura and Okabe (2013) also confirmed the predominance of *Geobacter* sp. as acetoclastic exoelectrogens in BES. The direct interspecies electron transfer (DIET) may be associated with the processes of *Geobacter* and other EAMs in utilizing acetate to conducted electricity (Cheng and Call 2016). Considering the existence of *Pseudomonas* in biofilm and suspension, phenazines produced by *Pseudomonas* can also transfer the electrons from the oxidation of acetate to the anode (Pham et al., 2008; Rabaey et al., 2005), as revealed by the cyclic voltammetry result (Figure S11). This indirect electron transfer mechanism can promote redox interactions for the microbial community and increase the performance of anode biofilms (Cheng and Call 2016). It can be suggested that acetate, rather than BPS, served as an electron donor for electricity generation by EAMs during BPS degradation in this study.

To date, this is the first study investigating the network among microbes with different functions in the bioelectrochemical degradation of pollutants, which can provide information on what microbes are physically and/or functionally associated in a microbial community (Zhou et al., 2011). EAMs cannot directly degrade contaminants but utilize their metabolites (Borole et al., 2011; Cheng and Call 2016), which refers to the metabolites mediated interspecies electron transfer (MIET). Considering acetate and other low-molecular byproducts can also be transformed from BPS (Figure 3), the removal of these simple organic products such as acetate by EAMs and other synergistic microbes theoretically reduces potential feedback inhibition effects (Kiely et al., 2011), thereby accelerate the biodegradation of BPS. These presumptions can also explain the intense microbial networks between EAMs and the non-EAMs (including BPS assimilators) that observed in biofilms. Therefore, this MIET-based syntrophic interaction and the DIET-based electrochemical interaction collectively established the redox equilibrium in bioelectrochemically enhanced degradation of BPS.

Moreover, SIAM was used to identify hydrolysis and oxidation processes as the initial and key transformation pathways for bioelectrochemical degradation; followed by the hydroxylation of one or two phenolic rings, aromatic ring cleavage, or alkylation in the formation of highly (but not fully) isotopic products. These isotopic-validated pathways were similar to those in aerobic degradation of BPS in sludge and sediment (Choi and Lee 2017; Huang et al., 2019; Kovačič et al., 2021; Ogata et al., 2013), including hydrolysis, methylation, cleavage and the coupling of smaller bisphenol moieties. A recent study on other BP analogs degradation by bacteria also reported for the common biodegradation pathways (Noszczyńska and Piotrowska-Seget 2018). Previous studies also confirmed the possibility of dihydroxybenzene transformation to benzoquinone, diene acid, benzoic acid, and aromatic ring-cleavage products by EAMs (Milligan and Häggblom 1998; Su et al., 2019; Uchimiya and Stone 2006; Zhou et al., 2020). Hence, we can propose that the driving reaction with anode as electron acceptor can produce degradation pathways similar to those under aerobic reaction.

In the conventionally anaerobic condition, the biodegradation of organic compounds was highly dependent upon the presence of electron acceptors or electron donors (Berry et al., 1987). Previous studies indicated that the degradation pathways of recalcitrant substances in BES may be directly dependent on degradation of the anode or cathode, which has been illustrated to be used as a sole electron acceptor or donor in BES (Huang et al., 2011; Logan 2009; Strycharz et al., 2010). Sun et al. (2019) proposed that the deoxidation of sulfone (lost oxygen atoms) and the following C-S bond cleavage were the two common transformation pathways for BPS under anaerobic conditions and in BES cathode, which was quite different from the present study. It can be explained by the cathodic degradation of BPS in their study caused by the application of negative anodic potential. The influence of the applied potential on the degradation pathways of recalcitrant substances has also been investigated by several studies (Feng et al., 2017; Strycharz et al. 2008, 2010). Therefore, we speculate that the BPS degradation pathways in BES were stable under different positive potentials in the present study (from 0.2V to 0.6V).

SIP techniques offer an excellent opportunity to identify new unexpected degradation pathways and reveal hidden metabolic mechanisms. This work illustrates the potential of using SIP techniques to study the bioelectrochemical degradation mechanisms of pollutants, which strengthens the promise of integrating two stable isotopic approaches in BES platforms. The proposed unique microbial cooperation mechanism in

electroactive biofilm provides new insights into the enhanced degradation mechanisms in BES for several other structure-similar pollutants. This research can also beneficially inform the design of EAB structures and the development of specific engineered assimilators for BESs in future wastewater treatment applications.

Limitations of the study

However, this study only tracked the short-term process from BPS to primary degradation products in BES using stable isotope. Future work covering long-term investigation on the stable isotope dynamics during entire contaminant assimilation process (from BPS to inorganic carbon) is needed to disclose more detailed and reliable fundamental information related to metabolic and redox interactions in BESs for pollutants remediation.

Resource availability

Lead contact

Further information and requests for resources and reagents should be directed to and will be fulfilled by the lead contact, Prof. Yong Yuan (yuanyong@soil.gd.cn).

Materials availability

This study did not generate new unique reagents.

Data and code availability

This study did not generate datasets/code.

METHODS

All methods can be found in the accompanying Transparent Methods supplemental file.

SUPPLEMENTAL INFORMATION

Supplemental Information can be found online at https://doi.org/10.1016/j.isci.2020.102014.

ACKNOWLEDGMENTS

This study was supported jointly by the National Natural Science Foundation of China (Nos. 41877045, 41907339 and 21876032) and China Postdoctoral Research Funds (No. 2018M640765).

AUTHOR CONTRIBUTIONS

Conceptualization: Rui Hou and Yong Yuan; Methodology and Investigation: Rui Hou, Lin Gan, and Jibing Li: Writing – Original Draft: Rui Hou; Methodology: Yi Wang and Jibing Li; Writing – Review & Editing: Yong Yuan and Shungui Zhou; Funding Acquisition: Yong Yuan; Resources: Yong Yuan and Jibing Li; Supervision: Yong Yuan and Shungui Zhou.

DECLARATION OF INTERESTS

The authors declare no competing interests.

Received: August 31, 2020
Revised: December 3, 2020
Accepted: December 24, 2020
Published: January 22, 2021

REFERENCES

Badia-Fabregat, M., Rosell, M., Caminal, G., Vicent, T., and Marco-Urrea, E. (2014). Use of stable isotope probing to assess the fate of emerging contaminants degraded by white-rot fungus. Chemosphere *103*, 336–342.

Baran, R., Bowen, B.P., Bouskill, N.J., Brodie, E.L., Yannone, S.M., and Northen, T.R. (2010). Metabolite identification in Synechococcus sp. PCC 7002 using untargeted stable isotope assisted metabolite profiling. Anal. Chem. *82*, 9034–9042.

Bernard, L., Mougel, C., Maron, P.A., Nowak, V., Lévêque, J., Henault, C., Haichar, F.E.Z., Berge, O., Marol, C., and Balesdent, J. (2007). Dynamics and identification of soil microbial populations actively assimilating carbon from 13C-labelled wheat residue as estimated by DNA- and RNA-SIP techniques. Environ. Microbiol. *9*, 752–764.

Berry, D.F., Francis, A.J., and Bollag, J.M. (1987). Microbial metabolism of homocyclic and heterocyclic aromatic compounds under anaerobic conditions. Microbiol. Rev. *51*, 43–59.

Bhute, S.S., Escobedo, B., Haider, M., Mekonen, Y., Ferrer, D., Hillyard, S.D., Friel, A.D., van Breukelen, F., and Hedlund, B.P. (2020). The gut microbiome and its potential role in paradoxical anaerobism in pupfishes of the Mojave Desert. Anim. Microbiome *2*, 20.

Borole, A.P., Reguera, G., Ringeisen, B., Wang, Z.-W., Feng, Y., and Kim, B.H. (2011). Electroactive biofilms: current status and future research needs. Energy Environ. Sci. *4*, 4813–4834.

Bueschl, C., Kluger, B., Neumann, N.K.N., Doppler, M., Maschietto, V., Thallinger, G.G., Meng-Reiterer, J., Krska, R., and Schuhmacher, R. (2017). MetExtract II: a software suite for stable isotope-assisted untargeted metabolomics. Anal. Chem. *89*, 9518–9526.

Call, D.F., Wagner, R.C., and Logan, B.E. (2009). Hydrogen production by Geobacter species and a mixed consortium in a microbial electrolysis cell. Appl. Environ. Microbiol. *75*, 7579.

Cao, M., Feng, Y., Wang, N., Li, Y., Li, N., Liu, J., and He, W. (2020). Electrochemical regulation on the metabolism of anode biofilms under persistent exogenous bacteria interference. Electrochim. Acta *340*, 135922.

Cao, Z., Zhang, M., Zhang, J., and Zhang, H. (2016). Impact of continuous and intermittent supply of electric assistance on high-strength 2,4-dichlorophenol (2,4-DCP) degradation in electro-microbial system. Bioresour. Technol. *212*, 138–143.

Capellades, J., Navarro, M., Samino, S., Garcia-Ramirez, M., Hernandez, C., Simo, R., Vinaixa, M., and Yanes, O. (2016). geoRge: a computational tool to detect the presence of stable isotope labeling in LC/MS-based untargeted metabolomics. Anal. Chem. *88*, 621–628.

Chae, K.-J., Choi, M.-J., Lee, J.-W., Kim, K.-Y., and Kim, I.S. (2009). Effect of different substrates on the performance, bacterial diversity, and bacterial viability in microbial fuel cells. Bioresour. Technol. *100*, 3518–3525.

Chen, D., Kannan, K., Tan, H., Zheng, Z., Feng, Y.-L., Wu, Y., and Widelka, M. (2016). Bisphenol analogues other than BPA: environmental occurrence, human exposure, and toxicity—a review. Environ. Sci. Technol. *50*, 5438–5453.

Cheng, Q., and Call, D.F. (2016). Hardwiring microbes via direct interspecies electron transfer: mechanisms and applications. Environ. Sci. Process. Impacts *18*, 968–980.

Choi, Y.J., and Lee, L.S. (2017). Aerobic soil biodegradation of bisphenol (BPA) alternatives bisphenol S and bisphenol AF compared to BPA. Environ. Sci. Technol. *51*, 13698–13704.

Comte, S., Guibaud, G., and Baudu, M. (2006). Relations between extraction protocols for activated sludge extracellular polymeric substances (EPS) and EPS complexation properties: Part I. Comparison of the efficiency of eight EPS extraction methods. Enzyme Microb. Technol. *38*, 237–245.

Creek, D.J., Chokkathukalam, A., Jankevics, A., Burgess, K.E.V., Breitling, R., and Barrett, M.P. (2012). Stable isotope-assisted metabolomics for network-wide metabolic pathway elucidation. Anal. Chem. *84*, 8442–8447.

Creek, D.J. (2013). Stable isotope labeled metabolomics improves identification of novel metabolites and pathways. Bioanalysis *5*, 1807–1810.

Daghio, M., Espinoza Tofalos, A., Leoni, B., Cristiani, P., Papacchini, M., Jalilnejad, E., Bestetti, G., and Franzetti, A. (2018). Bioelectrochemical BTEX removal at different voltages: assessment of the degradation and characterization of the microbial communities. J. Hazard. Mater. *341*, 120–127.

Dumont, M.G., and Murrell, J.C. (2005). Stable isotope probing — linking microbial identity to function. Nat. Rev. Microbiol. *3*, 499–504.

Fan, M., Zhou, N., Li, P., Chen, L., Chen, Y., Shen, S., and Zhu, S. (2017). Anaerobic co-metabolic biodegradation of tetrabromobisphenol A using a bioelectrochemical system. J. Hazard. Mater. *321*, 791–800.

Feng, H., Wang, Y., Zhang, X., Shen, D., Li, N., Chen, W., Huang, B., Liang, Y., and Zhou, Y. (2017). Degradation of p-fluoronitrobenzene in biological and bioelectrochemical systems: differences in kinetics, pathways, and microbial community evolutions. Chem. Eng. J. *314*, 232–239.

Fernando, E.Y., Keshavarz, T., and Kyazze, G. (2019). The use of bioelectrochemical systems in environmental remediation of xenobiotics: a review. J. Chem. Technol. Biotechnol. *94*, 2070–2080.

Ha, P.T., Lee, T.K., Rittmann, B.E., Park, J., and Chang, I.S. (2012). Treatment of alcohol distillery wastewater using a bacteroidetes-dominant thermophilic microbial fuel cell. Environ. Sci. Technol. *46*, 3022–3030.

Hao, Y.T., Wu, S.G., Jakovlić, I., Zou, H., Li, W.X., and Wang, G.T. (2017). Impacts of diet on hindgut microbiota and short-chain fatty acids in grass carp (Ctenopharyngodon idellus). Aquac. Res. *48*, 5595–5605.

Hasany, M., Mardanpour, M.M., and Yaghmaei, S. (2016). Biocatalysts in microbial electrolysis cells: a review. Int. J. Hydrogen Energy *41*, 1477–1493.

Hou, R., Luo, X., Liu, C., Zhou, L., Wen, J., and Yuan, Y. (2019). Enhanced degradation of triphenyl phosphate (TPHP) in bioelectrochemical systems: kinetics, pathway and degradation mechanisms. Environ. Pollut. *254*, 113040.

Huang, L., Cheng, S., and Chen, G. (2011). Bioelectrochemical systems for efficient recalcitrant wastes treatment. J. Chem. Technol. Biotechnol. *86*, 481–491.

Huang, W.-C., Jia, X., Li, J., and Li, M. (2019). Dynamics of microbial community in the bioreactor for bisphenol S removal. Sci. Total Environ. *662*, 15–21.

Ji, J., Kulshreshtha, S., Kakade, A., Majeed, S., Li, X., and Liu, P. (2020). Bioaugmentation of membrane bioreactor with Aeromonas hydrophila LZ-MG14 for enhanced malachite green and hexavalent chromium removal in textile wastewater. Int. Biodeterior. Biodegradation *150*, 104939.

Jia, J., Tang, Y., Liu, B., Wu, D., Ren, N., and Xing, D. (2013). Electricity generation from food wastes and microbial community structure in microbial fuel cells. Bioresour. Technol. *144*, 94–99.

Jones, M.D., Crandell, D.W., Singleton, D.R., and Aitken, M.D. (2011). Stable-isotope probing of the polycyclic aromatic hydrocarbon-degrading bacterial guild in a contaminated soil. Environ. Microbiol. *13*, 2623–2632.

Kästner, M., Streibich, S., Beyrer, M., Richnow, H.H., and Fritsche, W. (1999). formation of bound residues during microbial degradation of [^{14}C] anthracene in soil. Appl. Environ. Microbiol. *65*, 1834–1842.

Kang, F., Alvarez, P.J., and Zhu, D. (2014). Microbial extracellular polymeric substances reduce Ag+ to silver nanoparticles and antagonize bactericidal activity. Environ. Sci. Technol. *48*, 316–322.

Kiely, P.D., Regan, J.M., and Logan, B.E. (2011). The electric picnic: synergistic requirements for exoelectrogenic microbial communities. Curr. Opin. Biotechnol. *22*, 378–385.

Kimura, Z.-i., and Okabe, S. (2013). Acetate oxidation by syntrophic association between Geobacter sulfurreducens and a hydrogen-utilizing exoelectrogen. ISME J. *7*, 1472–1482.

Kovačič, A., Gys, C., Kosjek, T., Covaci, A., and Heath, E. (2019). Photochemical degradation of BPF, BPS and BPZ in aqueous solution: identification of transformation products and degradation kinetics. Sci. Total Environ. *664*, 595–604.

Kovačič, A., Gys, C., Gulin, M.R., Gornik, T., Kosjek, T., Heath, D., Covaci, A., and Heath, E. (2021). Kinetics and biotransformation products of bisphenol F and S during aerobic degradation with activated sludge. J. Hazard. Mater. *404*, 124079.

Lee, D.G., Cho, K.-C., and Chu, K.-H. (2014). Identification of triclosan-degrading bacteria in a triclosan enrichment culture using stable isotope probing. Biodegradation *25*, 55–65.

Li, D.B., Huang, Y.X., Li, J., Li, L.L., Tian, L.J., and Yu, H.Q. (2017a). Electrochemical activities of Geobacter biofilms growing on electrodes with various potentials. Electrochim. Acta *225*, 452–457.

Li, H., Zhang, S., Yang, X.-L., Yang, Y.-L., Xu, H., Li, X.-N., and Song, H.-L. (2019). Enhanced degradation of bisphenol A and ibuprofen by an up-flow microbial fuel cell-coupled constructed wetland and analysis of bacterial community structure. Chemosphere *217*, 599–608.

Li, J., Luo, C., Song, M., Dai, Q., Jiang, L., Zhang, D., and Zhang, G. (2017b). Biodegradation of phenanthrene in polycyclic aromatic hydrocarbon-contaminated wastewater revealed by coupling cultivation-dependent and -independent approaches. Environ. Sci. Technol. *51*, 3391–3401.

Logan, B.E. (2009). Exoelectrogenic bacteria that power microbial fuel cells. Nat. Rev. Microbiol. *7*, 375–381.

Logan, B.E., Rossi, R., Ragab, A.a., and Saikaly, P.E. (2019). Electroactive microorganisms in bioelectrochemical systems. Nat. Rev. Microbiol. *17*, 307–319.

Lovley, D.R. (2011). Live wires: direct extracellular electron exchange for bioenergy and the bioremediation of energy-related contamination. Energy Environ. Sci. *4*, 4896–4906.

Lu, L., Huggins, T., Jin, S., Zuo, Y., and Ren, Z.J. (2014). Microbial metabolism and community structure in response to bioelectrochemically enhanced remediation of petroleum hydrocarbon-contaminated soil. Environ. Sci. Technol. *48*, 4021–4029.

Luo, C., Hou, R., Chen, G., Liu, C., Zhou, L., and Yuan, Y. (2019). UVC-assisted electrochemical degradation of novel bisphenol analogues with boron-doped diamond electrodes: kinetics, pathways and eco-toxicity removal. Sci. Total Environ. *711*, 134539.

Luo, H., Liu, G., Zhang, R., and Jin, S. (2009). Phenol degradation in microbial fuel cells. Chem. Eng. J. *147*, 259–264.

Milligan, P.W., and Häggblom, M.M. (1998). Biodegradation of resorcinol and catechol by denitrifying enrichment cultures. Environ. Toxicol. Chem. *17*, 1456–1461.

Miran, W., Jang, J., Nawaz, M., Shahzad, A., and Lee, D.S. (2018). Biodegradation of the sulfonamide antibiotic sulfamethoxazole by sulfamethoxazole acclimatized cultures in microbial fuel cells. Sci. Total Environ. *627*, 1058–1065.

Motteran, F., Braga, J.K., Silva, E.L., and Varesche, M.B.A. (2016). Influence of sucrose on the diversity of bacteria involved in nonionic surfactant degradation in fluidized bed reactor. Water Air Soil Pollut. *228*, 21.

Motteran, F., Okada, D.Y., Delforno, T.P., and Varesche, M.B.A. (2020). Influence of cosubstrates for linear anionic sulfonated alkylbenzene degradation and methane production in anaerobic batch reactors. Process Saf. Environ. Prot. *139*, 60–68.

Ng, I.S., Hsueh, C.-C., and Chen, B.-Y. (2017). Electron transport phenomena of electroactive bacteria in microbial fuel cells: a review of Proteus hauseri. Bioresourc. Bioprocess. *4*, 53.

Noszczyńska, M., and Piotrowska-Seget, Z. (2018). Bisphenols: application, occurrence, safety, and biodegradation mediated by bacterial communities in wastewater treatment plants and rivers. Chemosphere *201*, 214–223.

Ogata, Y., Goda, S., Toyama, T., Sei, K., and Ike, M. (2013). The 4-tert-Butylphenol-Utilizing bacterium sphingobium fuliginis OMI can degrade bisphenols via phenolic ring hydroxylation and meta-cleavage pathway. Environ. Sci. Technol. *47*, 1017–1023.

Pellis, A., Cantone, S., Ebert, C., and Gardossi, L. (2018). Evolving biocatalysis to meet bioeconomy challenges and opportunities. New Biotechnol. *40*, 154–169.

Pham, H., Boon, N., Marzorati, M., and Verstraete, W. (2009). Enhanced removal of 1,2-dichloroethane by anodophilic microbial consortia. Water Res. *43*, 2936–2946.

Pham, T.H., Boon, N., De Maeyer, K., Höfte, M., Rabaey, K., and Verstraete, W. (2008). Use of Pseudomonas species producing phenazine-based metabolites in the anodes of microbial fuel cells to improve electricity generation. Appl. Microbiol. Biotechnol. *80*, 985–993.

Rabaey, K., Boon, N., Höfte, M., and Verstraete, W. (2005). Microbial phenazine production enhances electron transfer in biofuel cells. Environ. Sci. Technol. *39*, 3401–3408.

Rabaey, K., and Rozendal, R.A. (2010). Microbial electrosynthesis — revisiting the electrical route for microbial production. Nat. Rev. Microbiol. *8*, 706–716.

Rismani-Yazdi, H., Carver, S.M., Christy, A.D., Yu, Z., Bibby, K., Peccia, J., and Tuovinen, O.H. (2013). Suppression of methanogenesis in cellulose-fed microbial fuel cells in relation to performance, metabolite formation, and microbial population. Bioresour. Technol. *129*, 281–288.

Ruth, R.J., and Louise, B.A. (2015). Bisphenol S and F: a systematic review and comparison of the hormonal activity of bisphenol A substitutes. Environ. Health Perspect. *123*, 643–650.

Saratale, G.D., Saratale, R.G., Shahid, M.K., Zhen, G., Kumar, G., Shin, H.-S., Choi, Y.-G., and Kim, S.-H. (2017). A comprehensive overview on electro-active biofilms, role of exo-electrogens and their microbial niches in microbial fuel cells (MFCs). Chemosphere *178*, 534–547.

Sathyamoorthy, S., Hoar, C., and Chandran, K. (2018). Identification of bisphenol A-assimilating microorganisms in mixed microbial communities using 13C-DNA stable isotope probing. Environ. Sci. Technol. *52*, 9128–9135.

Schymanski, E.L., Jeon, J., Gulde, R., Fenner, K., Ruff, M., Singer, H.P., and Hollender, J. (2014). Identifying small molecules via high resolution mass spectrometry: communicating confidence. Environ. Sci. Technol. *48*, 2097–2098.

Shehab, N.A., Ortiz-Medina, J.F., Katuri, K.P., Hari, A.R., Amy, G., Logan, B.E., and Saikaly, P.E. (2017). Enrichment of extremophilic exoelectrogens in microbial electrolysis cells using Red Sea brine pools as inocula. Bioresour. Technol. *239*, 82–86.

Sheng, G.-P., Yu, H.-Q., and Li, X.-Y. (2010). Extracellular polymeric substances (EPS) of microbial aggregates in biological wastewater treatment systems: a review. Biotechnol. Adv. *28*, 882–894.

Song, L., Wang, Y., Tang, W., and Lei, Y. (2015a). Bacterial community diversity in municipal waste landfill sites. Appl. Microbiol. Biotechnol. *99*, 7745–7756.

Song, M., Jiang, L., Zhang, D., Luo, C., Wang, Y., Yu, Z., Yin, H., and Zhang, G. (2016). Bacteria capable of degrading anthracene, phenanthrene, and fluoranthene as revealed by DNA based stable-isotope probing in a forest soil. J. Hazard. Mater. *308*, 50–57.

Song, Y., Xiao, L., Jayamani, I., He, Z., and Cupples, A.M. (2015b). A novel method to characterize bacterial communities affected by carbon source and electricity generation in microbial fuel cells using stable isotope probing and Illumina sequencing. J. Microbiol. Methods *108*, 4–11.

Srikanth, S., Kumar, M., Singh, D., Singh, M.P., Puri, S.K., and Ramakumar, S.S.V. (2018). Long-term operation of electro-biocatalytic reactor for carbon dioxide transformation into organic molecules. Bioresour. Technol. *265*, 66–74.

Strycharz, S.M., Woodard, T.L., Johnson, J.P., Nevin, K.P., Sanford, R.A., Löffler, F.E., and Lovley, D.R. (2008). Graphite electrode as a sole electron donor for reductive dechlorination of tetrachlorethene by Geobacter lovleyi</em&gt. Appl. Environ. Microbiol. *74*, 5943.

Strycharz, S.M., Gannon, S.M., Boles, A.R., Franks, A.E., Nevin, K.P., and Lovley, D.R. (2010). Reductive dechlorination of 2-chlorophenol by Anaeromyxobacter dehalogenans with an electrode serving as the electron donor. Environ. Microbiol. Rep. *2*, 289–294.

Su, C., Lu, Y., Deng, Q., Chen, S., Pang, G., Chen, W., Chen, M., and Huang, Z. (2019). Performance of a novel ABR-bioelectricity-Fenton coupling reactor for treating traditional Chinese medicine wastewater containing catechol. Ecotoxicol. Environ. Saf. *177*, 39–46.

Sun, J., Xu, Y., Jiang, L., Fan, M., Xu, H., Chen, Y., and Shen, S. (2019). Highly efficient transformation of bisphenol S by anaerobic cometabolism in the bioelectrochemical system. J. Environ. Eng. *145*, 04019079.

Tian, X., Song, Y., Shen, Z., Zhou, Y., Wang, K., Jin, X., Han, Z., and Liu, T. (2020). A comprehensive review on toxic petrochemical wastewater pretreatment and advanced treatment. J. Clean. Prod. *245*, 118692.

Tian, Z., Vila, J., Yu, M., Bodnar, W., and Aitken, M.D. (2018). Tracing the biotransformation of polycyclic aromatic hydrocarbons in contaminated soil using stable isotope-assisted metabolomics. Environ. Sci. Technol. Lett. *5*, 103–109.

Uchimiya, M., and Stone, A.T. (2006). Aqueous oxidation of substituted dihydroxybenzenes by substituted benzoquinones. Environ. Sci. Technol. *40*, 3515–3521.

Wang, L., Liu, Y., Ma, J., and Zhao, F. (2016). Rapid degradation of sulphamethoxazole and the further transformation of 3-amino-5-methylisoxazole in a microbial fuel cell. Water Res. *88*, 322–328.

Wang, Q., Lu, X., Cao, Y., Ma, J., Jiang, J., Bai, X., and Hu, T. (2017). Degradation of Bisphenol S by heat activated persulfate: kinetics study, transformation pathways and influences of co-existing chemicals. Chem. Eng. J. *328*, 236–245.

Wei, L., Li, J., Xue, M., Wang, S., Li, Q., Qin, K., Jiang, J., Ding, J., and Zhao, Q. (2019). Adsorption behaviors of Cu2+, Zn2+ and Cd2+ onto proteins, humic acid, and polysaccharides extracted from sludge EPS: sorption properties and mechanisms. Bioresour. Technol. *291*, 121868.

Xu, H., Tong, N., Huang, S., Zhou, S., Li, S., Li, J., and Zhang, Y. (2018). Degradation of 2,4,6-trichlorophenol and determination of bacterial

community structure by micro-electrical stimulation with or without external organic carbon source. Bioresour. Technol. *263*, 266–272.

Yan, W., Xiao, Y., Yan, W., Ding, R., Wang, S., and Zhao, F. (2019). The effect of bioelectrochemical systems on antibiotics removal and antibiotic resistance genes: a review. Chem. Eng. J. *358*, 1421–1437.

Yan, Z., He, Y., Cai, H., Van Nostrand, J.D., He, Z., Zhou, J., Krumholz, L.R., and Jiang, H.-L. (2017). Interconnection of key microbial functional genes for enhanced benzo[a]pyrene biodegradation in sediments by microbial electrochemistry. Environ. Sci. Technol. *51*, 8519–8529.

Yang, G., Huang, L., Yu, Z., Liu, X., Chen, S., Zeng, J., Zhou, S., and Zhuang, L. (2019). Anode potentials regulate Geobacter biofilms: new insights from the composition and spatial structure of extracellular polymeric substances. Water Res. *159*, 294–301.

Yang, T.H., Coppi, M.V., Lovley, D.R., and Sun, J. (2010). Metabolic response of Geobacter sulfurreducens towards electron donor/acceptor variation. Microb. Cell Fact. *9*, 90.

Yang, Y., Xu, M., Guo, J., and Sun, G. (2012). Bacterial extracellular electron transfer in bioelectrochemical systems. Process Biochem. *47*, 1707–1714.

Zakaria, B.S., and Dhar, B.R. (2020). Changes in syntrophic microbial communities, EPS matrix, and gene-expression patterns in biofilm anode in response to silver nanoparticles exposure. Sci. Total Environ. *734*, 139395.

Zemb, O., Lee, M., Gutierrez-Zamora, M.L., Hamelin, J., Coupland, K., Hazrin-Chong, N.H., Taleb, I., and Manefield, M. (2012). Improvement of RNA-SIP by pyrosequencing to identify putative 4-n-nonylphenol degraders in activated sludge. Water Res. *46*, 601–610.

Zeng, X., Borole, A.P., and Pavlostathis, S.G. (2015). Biotransformation of furanic and phenolic compounds with hydrogen gas production in a microbial electrolysis cell. Environ. Sci. Technol. *49*, 13667–13675.

Zhan, Y., Liu, W., Bao, Y., Zhang, J., Petropoulos, E., Li, Z., Lin, X., and Feng, Y. (2018). Fertilization shapes a well-organized community of bacterial decomposers for accelerated paddy straw degradation. Sci. Rep. *8*, 7981.

Zhang, X., Feng, H., Shan, D., Shentu, J., Wang, M., Yin, J., Shen, D., Huang, B., and Ding, Y. (2014). The effect of electricity on 2–fluoroaniline removal in a bioelectrochemically assisted microbial system (BEAMS). Electrochim. Acta *135*, 439–446.

Zheng, Y., Xiao, Y., Yang, Z.-H., Wu, S., Xu, H.-J., Liang, F.-Y., and Zhao, F. (2014). The bacterial communities of bioelectrochemical systems associated with the sulfate removal under different pHs. Process Biochem. *49*, 1345–1351.

Zhou, J., Deng, Y., Luo, F., He, Z., and Yang, Y. (2011). Phylogenetic molecular ecological network of soil microbial communities in response to elevated CO<sub>2</sub&gt. mBio *2*, e00122–e00111.

Zhou, Y., Zou, Q., Fan, M., Xu, Y., and Chen, Y. (2020). Highly efficient anaerobic co-degradation of complex persistent polycyclic aromatic hydrocarbons by a bioelectrochemical system. J. Hazard. Mater. *381*, 120945.

iScience, Volume *24*

Supplemental Information

Bioelectrochemically enhanced degradation of bisphenol S: mechanistic insights from stable isotope-assisted investigations

Rui Hou, Lin Gan, Fengyi Guan, Yi Wang, Jibing Li, Shungui Zhou, and Yong Yuan

SUPPLEMENTAL INFORMATION

Bioelectrochemically enhanced degradation of bisphenol S: Mechanistic insights from stable isotope-assisted investigations

Rui Hou,[1] Lin Gan,[1] Fengyi Guan,[1] Yi Wang,[1] Jibing Li,[2] Shungui Zhou,[3] Yong Yuan[1,4,*]

[1] Guangzhou Key Laboratory Environmental Catalysis and Pollution Control, Guangdong Key Laboratory of Environmental Catalysis and Health Risk Control, School of Environmental Science and Engineering, Institute of Environmental Health and Pollution Control, Guangdong University of Technology, Guangzhou 510006, China

[2] State Key Laboratory of Organic Geochemistry, Guangzhou Institute of Geochemistry, Chinese Academy of Sciences, Guangzhou 510640, China

[3] Fujian Provincial Key Laboratory of Soil Environmental Health and Regulation, School of Resources and Environment, Fujian Agriculture and Forestry, Fuzhou 350000, China

[4] Lead Contact

***Correspondence**: yuanyong@soil.gd.cn (Y. Yuan).

Transparent Methods

Chemicals and reagents

Standards of BPS (4,4'-sulfonylbisphenol; CAS: 260408-02-4) and $^{13}C_{12}$-BPS (4,4'-sulfonylbisphenol-$^{13}C_{12}$) with isotopic purity > 99 % were purchased from Toronto Research Chemicals (Toronto, Canada). All solvents (HPLC grade) were purchased from Sigma-Aldrich (St. Louis, USA), and other used analytical-grade chemicals were purchased from Aladdin Industrial Corporation (Shanghai, China). Pure water (18.2 MΩ) was prepared using a Millipore Milli-Q system (Bedford, USA).

BES setup, operation and bioelectrode acclimation

Conventional three-electrode single chamber BES reactors were used for the degradation of BPS. Graphite plates (1.0 × 2.0 cm) and a titanium wire were used as the working and counter electrodes, respectively, and a saturated calomel electrode (SCE) was used as the reference electrode; the reactors were assembled into 100 mL cylindrical glass containers with a polytetrafluoroethylene lid. The effluent from a previously established well-operating BES was used as the inoculum (Yuan et al. 2011), and the reactors were operated at a potential of 0.2 V vs SCE at the working electrode in duplicate at 30 ℃. A multichannel potentiostat (CHI 1000C, CH Instrument, Shanghai, China) was used to record the current generation of the BESs. The culture medium contained NaAc (1 g/L), NaH_2PO_4 $2H_2O$ (2.84 g/L), Na_2HPO_4 $\cdot 12H_2O$ (11.4 g/L), NH_4Cl (0.31 g/L), KCl (0.13 g/L), vitamin solution (10 mL/L), and mineral solution (10 mL/L) (pH = 6.8), and the medium was changed every 48 h. After one month of culture, a mixed culture medium containing 2 mg/L BPS was injected into the reactors. Nine cycles later, we observed that BPS could be rapidly removed from the BES, which suggested that the EABs achieved a stable stage in accelerated degradation of BPS (Figure S1).

Degradation kinetics experiment and quantitation of BPS

Three acclimatized reactors were randomly selected and operated under batch mode to elucidate the effects of an external carbon supply (0-2 g NaAc) and varying anode potentials (0-0.6 V) on BPS degradation, while another three reactor electrodes were autoclaved and set as abiotic controls (AC). At specified incubation times, aqueous samples were collected and extracted using 1:1 v/v methanol, passed through a 0.22 mm filter (GHP Acrodisc; PALL,

Dreieich, Germany), and immediately stored at -20 ℃ until analysis.

The concentrations of the BPS samples from the batch processes were determined using high-performance liquid chromatography (HPLC) with a UV detector (Essentia LC-16; Shimadzu, Osaka, Japan), following the methods from Sun et al. (2014) and Yang et al. (2019). The analytical column was a WondaSil C18 column (4.6 mm × 150 mm, 4 μm particle diameter), and a UV wavelength of 276 nm was used. The mobile phase consisted of 65:35 (v/v) ultrapure water and methanol at a flow rate of 1 mL/min. The BPS peak retention time was 2.5 min, the HPLC method limit of quantitation (MLOQ) was 0.028 mg/L, and showed fully quantitative recovery ranged from 92% to 103%.

Stable isotope-assisted metabolomics (SIAM) experiment

Prior to the SIAM batch experiment, culture medium containing BPS (1 mg/L) and $^{13}C_{12}$-BPS (1.024 mg/L) was transferred into the acclimatized reactors for more than three cycles to thoroughly minimize the adsorbed fraction of ^{12}C-BPS in the biofilm. All reactors contained a mixture of 50 % nonlabeled BPS and 50 % $^{13}C_{12}$-BPS as a stable isotope carbon source. Other incubation conditions were as described previously. After 48 h of incubation, aqueous samples were collected and extracted following to previous method (Baran et al. 2010, Doppler et al. 2016, Yuan et al. 2018). In brief, 2 mL of the culture medium was resuspended in 2 mL of methanol/acetonitrile mixtures (1:1 v/v) and sonicated for 1 min, the suspension was centrifuged at 2,000 g for 10 min and passed through a 0.22 mm filter (GHP Acrodisc; PALL, Dreieich, Germany), and the supernatant was immediately stored at -80 ℃ for future analysis.

Samples were analyzed using ultra-performance liquid chromatography Q-Exactive Orbitrap mass spectrometry (UPLC-q-Orbitrap MS, Thermo Fisher Scientific, CA, USA). MS^2 scan mode with electrospray ionization (ESI) was used for SIAM analysis, and product ion scanning (MS/MS) was applied to elucidate the putative structures of metabolites. Raw data from q-Orbitrap-MS were converted into mzXML format by MSConvert (Proteowizard, version 3.0.9987). Peak detection, alignment, deconvolution and isotope group picking were achieved using “All Extract” from MetExtract II software (Bueschl et al. 2017). The software automatically convoluted the coeluting ^{12}C and ^{13}C-labeled metabolite ions into feature groups, where each group represented a unique metabolite. The confirmation of the products was based on the

following criteria: (a) the isotopologue metabolites (M') and their ^{12}C counterparts (M) must be present in the same MS scan; (b) the *D*-values of the molecular weight (ΔMW) differences derived from isotopologue metabolites (M') and their ^{12}C counterparts (M) must be divisible by 1.0034u (± 0.0005); (c) the intensity ratio of M'/M is theoretically 1:1; and (d) M' and M pairs cannot be found in the abiotic control group (Bueschl et al. 2017). Final annotation and molecular formula assignment were achieved in ChemSpider by Compound Discoverer 2.0 (Thermo Scientific), and the MS/MS fragments were compared in the m/z Cloud database.

^{13}C-DNA stable isotope probing (DNA-SIP) experiment and high-throughput sequencing

Aqueous suspensions from the acclimatized BES reactors at the time of > 90 % removal of BPS were sampled and inoculated into new reactors with culture medium only containing 2 mg/L $^{13}C_{12}$-BPS. Considering that the majority of BPS was degraded by the microbes during the first 24 h (Figure 1-A), the incubation period for DNA-SIP batch experiments was set as 24 h, and the culture medium was completely replaced for each cycle to avoid cross-feeding. After 5 cycles of batch incubation, mature biofilms in the anode were achieved, and the biofilm and reactor suspension were sampled for the detection of ^{13}C-labeled microbes. Biofilm and reactor suspension samples amended with unlabeled BPS were also sacrificed for DNA extraction.

The microbial DNA was extracted from the biofilms and suspensions using the EZNA™ Mag-Bind Soil DNA Kit according to the instructions (OMEGA, GA, USA). After quantification, 5 μg of the extracted DNA from each treatment was subjected to stable isotope probing fractionation, according to Song et al. (2016) and Li et al. (2017). DNA was separated by ultracentrifugation at 178,000 g for 48 h at 20 °C using a CsCl solution with a final buoyant density (BD) of ~1.77 g/mL. Centrifuged gradients were fractionated from bottom to top into 10 equal fractions. The BD value for each fraction was measured, and the purified DNA was quantified using an ND-2000 ultraviolet-visible spectrophotometer (Nano Drop Technologies, Wilmington, DE, USA). For 16S rRNA gene amplicon sequencing, the V3-V4 region was amplified with the primers 341F and 805R, and the purified amplicons were analyzed on an Illumina MiSeq platform (Illumina, San Diego, USA) by Oebiotech Co. Ltd. (Shanghai, China). Raw data were uploaded as fastq files to Sequence Read Archive (SRA) under accession

number PRJNA686243. After screening, the sequence data for each operational taxonomic unit (OTU) were assigned using Usearch v5.2.236 with 97 % sequence identity. OTU data was analyzed using both an unsupervised principal coordinate analysis (PCoA) and a supervised partial least squares discriminant analysis (PLS-DA) to compare the beta-diversity between samples. Thirty-one OTU sequences with high average abundance in the biofilm and suspension samples have been deposited in the GenBank database under accession numbers MW287162-MW287192.

Molecular ecological network analysis

To understand the interactions among different microbial communities in the acclimated BESs during BPS degradation, a random matrix theory (RMT)-based approach was used to discern the changes in phylogenetic molecular ecological networks (pMENs) in the ^{12}C-BPS assimilated biofilm and suspension without fractionation based on community sequence data (Deng et al. 2012, Ling et al. 2016).

Phylogenetic molecular ecological networks (pMENs) offer a robust statistical means of analyzing networks as they provide solutions for common issues encountered in the use of high-throughput metagenomic data, including noise reduction and automatic network definition (Cao et al. 2011, Fernando et al. 2020). The following steps were used for the ecological network construction using MENAP (http://129.15.40.240/mena/): 1) A relative abundance (RA) matrix and an OTU annotation file were prepared as per the pipeline guidelines; 2) The RA matrix was submitted for network construction. A cut-off value (similarity threshold, *st*) for the similarity matrix was automatically generated using default settings; 3) Calculations of “global network properties”, “individual nodes' centrality”, and “module separation and modularity” were performed; 4) The “output for Cytoscape visualization” procedure was performed in “greedy modularity optimization mode”. The network graphs were visualized by Gephi software (Zhan et al. 2018); 5) The “randomize the network structure and then calculate network” procedure was performed to calculate random network properties while maintaining the same number of nodes and links as the empirical networks and using the Maslov-Sneppen procedure (Wagner et al. 2009, Yan et al. 2018).

Statistical analysis

All data presented in this study are the mean ± standard deviation (SD) values of three replicates. Statistical analysis was carried out by Origin 8.0 (Origin Lab Corporation). One-way ANOVA was used to evaluate significant differences among treatment groups. A *p*-value of 0.05 was considered the cutoff for statistical significance.

Table S1 Rate constants *k* of BPS degradation in the BES various sodium acetate concentrations and various anode potentials. Related to Figure 1.

Treatment	Anode potential (V)	NaAc concentrations (g/L)	*k* (min^{-1})	R^2	72 h BPS removal (%)
Abiotic control	-	1	-0.010 ± 0.008	0.91	15.1
Open-circle BES	-	1	0.009 ± 0.004	0.99	25.8
Close-circle BES Under various anode potentials	0	1	0.037 ± 0.003	0.99	55.9
	0.2	1	0.061 ± 0.003	1.00	91.7
	0.4	1	0.039 ± 0.009	0.99	94.6
	0.6	1	0.056 ± 0.012	0.94	90.4
Close-circle BES Under various NaAc concentrations	0.2	0	0.027 ± 0.003	0.99	68.7
	0.2	0.5	0.033 ± 0.002	1.00	84.6
	0.2	1	0.061 ± 0.003	1.00	91.7
	0.2	2	0.069 ± 0.016	0.98	89.8

Table S2. Topological properties of the empirical molecular ecological networks (MENs) of microbial communities and their associated random MENs. Related to Figure 4.

Treatments	Experimental networks							Random networks						
	No of OTUs	Total nodes	Total links	R^2 of power law	Average Connectivity (avgK)	Average geodesic distance (GD)	Average clustering coefficient (avgCC)	Modularity (No of modules)	Average geodesic distance (GD)	Average clustering coefficient (avgCC)	Density (D)	Transitivity (Trans)	Connectedness (Con)	Modularity
Biofilm	468	227	451	0.870	3.974	4.396	0.272	0.723(20)	3.598±0.046	0.037±0.009	0.020±0.000	0.050±0.007	0.934±0.032	0.461±0.008
Suspension	473	110	332	0.755	6.036	3.909	0.356	0.612(24)	3.444±0.041	0.043±0.007	0.022±0.000	0.063±0.006	0.924±0.031	0.416±0.007

Table S3. Different microbial diversity indices of the different treatments. Related to Figure 4.

Samples	Reads	OTUs	Chao1	Coverage	Shannon	Simpson
Ini. biofilm	35312	9202	983.7096	0.986	4.33	0.903
Ini. suspension	34805	9202	650.3161	0.990	4.26	0.886
Accli. biofilm	38989	9202	695.4932	0.990	2.73	0.618
Accli. suspension	35410	9202	802.4755	0.988	4.29	0.900

Figure S1. Performance of BES during initial 9 cycles of acclimation with BPS as substrate.
(A) Current density in BES;
(B) 48 h degradation ratios in the BES.
Test conditions: sodium acetate 1.0 g/L, BPS 2 mg/L, external voltage 0.2 V, ambient temperature (28 ± 2 °C), pH=7.0. Related to Figure 1.

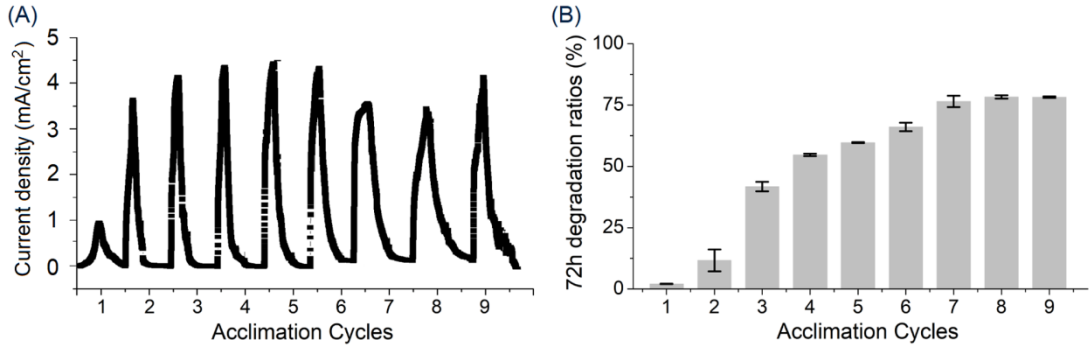

Figure S2. Current density in the BES during BPS degradation under various conditions.
(A) Current density under various NaAc concentrations;
(B) Current density under various anode potentials.
Test conditions: BPS 2 mg/L, ambient temperature (28 ±2 °C), pH=7.0. Related to Figure 1.

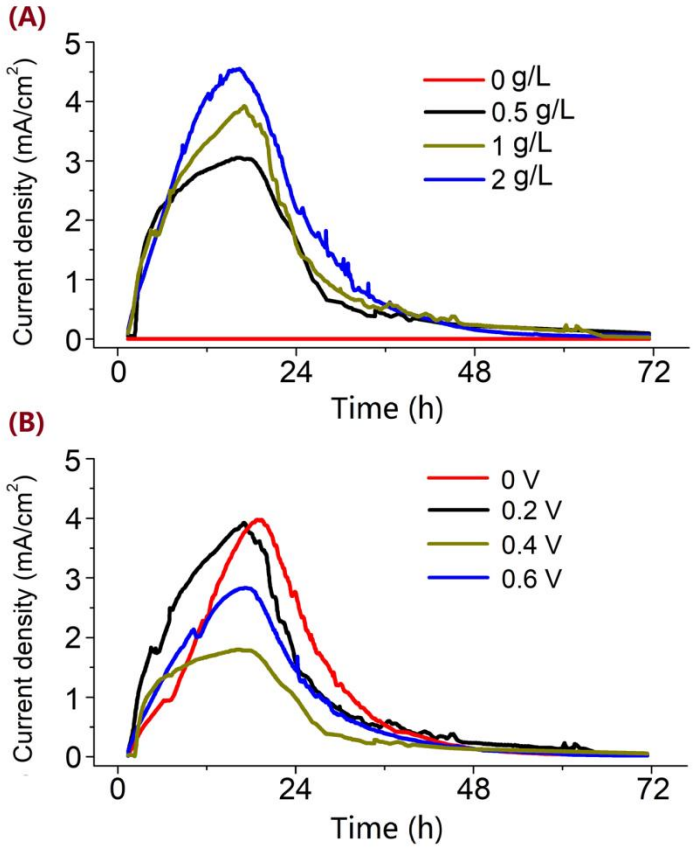

Figure S3. Chromatograms and MS spectra for the extracted native and ^{13}C labeled precursor ions of the analyzed feature groups (Fg1-3). Related to Figure 2.

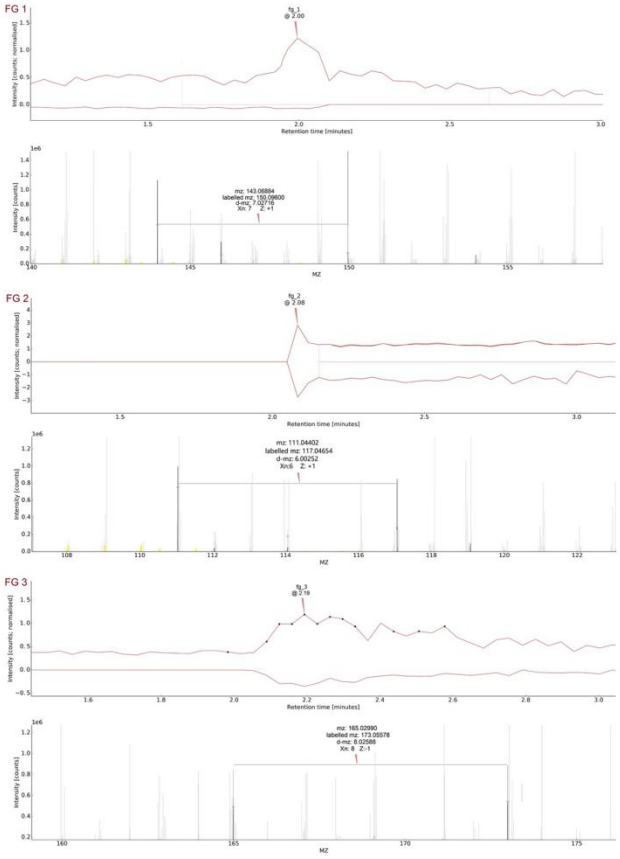

Figure S4. Chromatograms and MS spectra for the extracted native and ^{13}C labeled precursor ions of the analyzed feature groups (Fg4-6). Related to Figure 2.

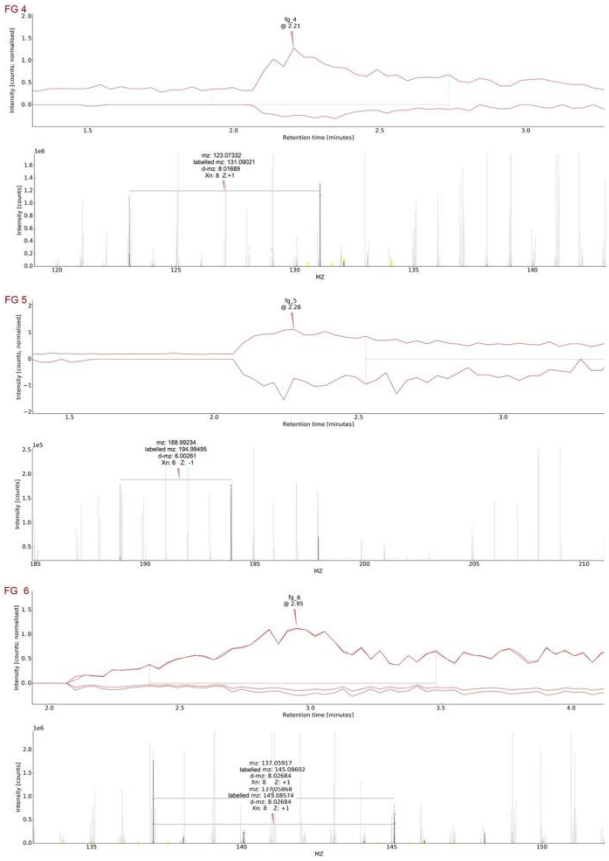

Figure S5. Chromatograms and MS spectra for the extracted native and ^{13}C labeled precursor ions of the analyzed feature groups (Fg7-9). Related to Figure 2.

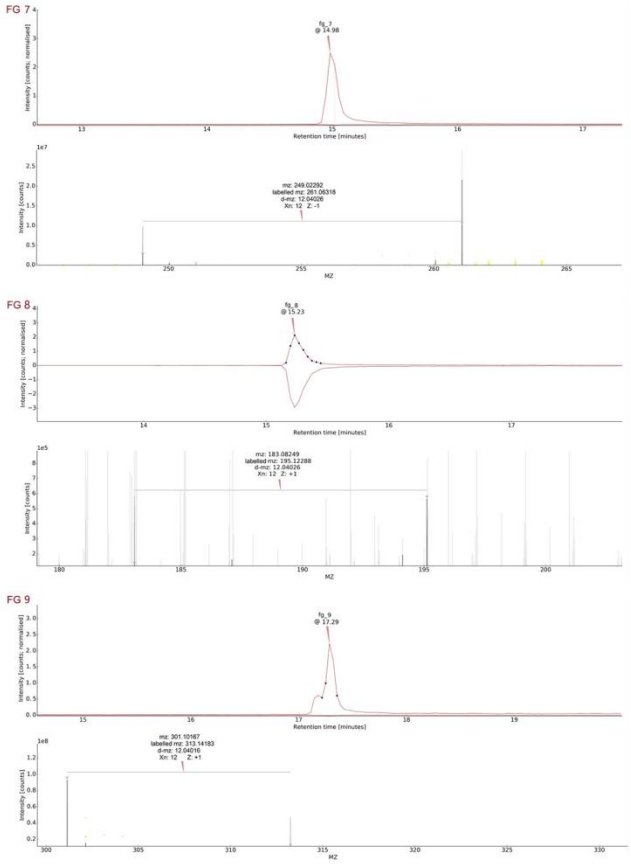

Figure S6. Fragmentation of chemically labeled products.

A: Triacetylmethane; B: Dihydroxybenzene; C: Terephthalic acid; D: BPS; and E: 2,2-dibenzyl-1,3-dithiane. Related to Figure 3.

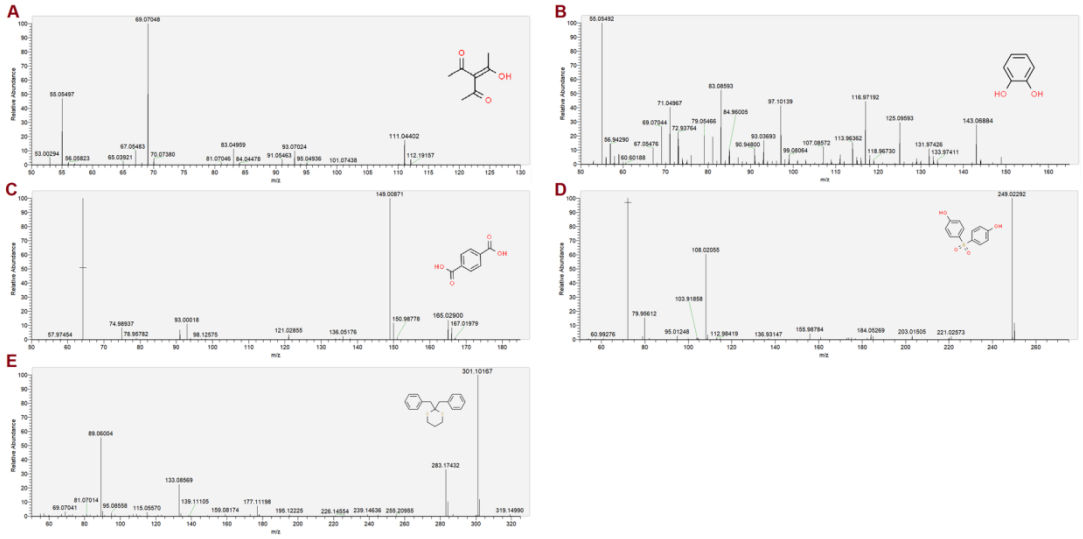

Figure S7. Correlation between DNA concentration (μg/mL) and buoyant density (g/mL) of the DNA fractions from the ^{12}C- and ^{13}C-BPS acclimatized biofilm and suspension. Related to Figure 5.

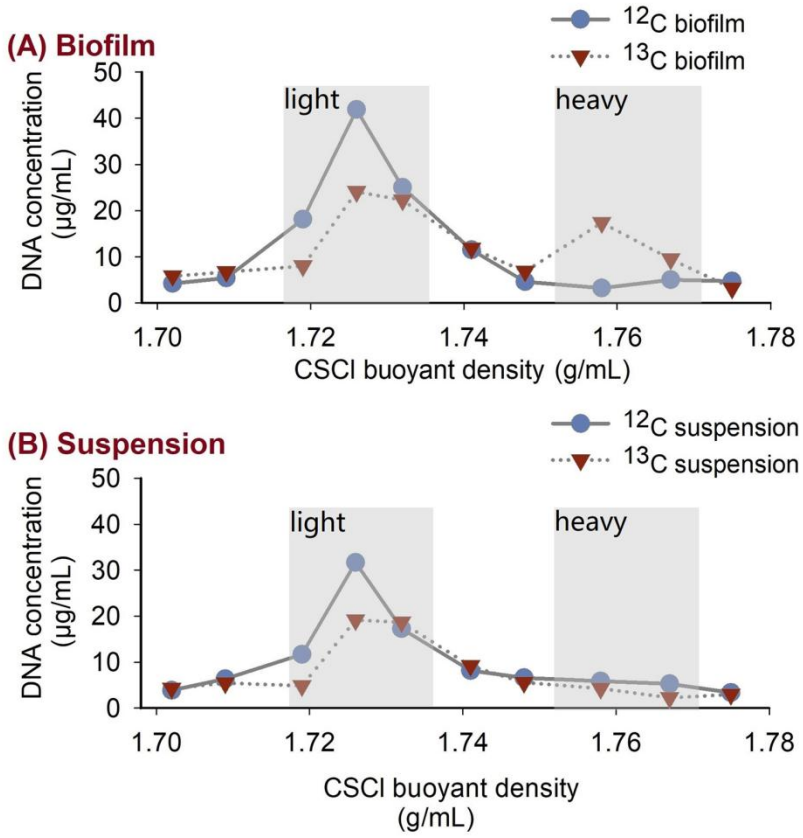

Figure S8. Relative abundances of different bacteria phylum and clas in the initial (Ini.) and acclimated (Accli.) anode biofilm and suspension and the light and heavy fractions from the ^{12}C and ^{13}C experiment. Related to Figure 4.

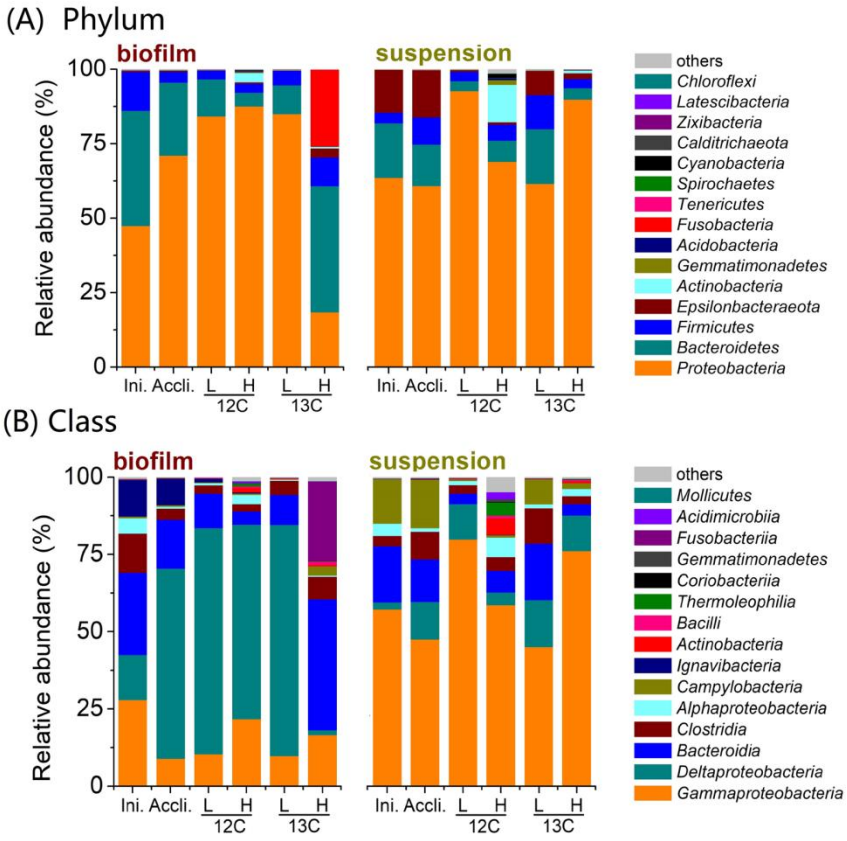

Figure S9. Zi-Pi plots showing the topological distribution of OTUs in the biofilm and suspension bacterial networks.

The keystone species (module hubs and connectors) are marked by OTU number and taxonomy. Related to Figure 4.

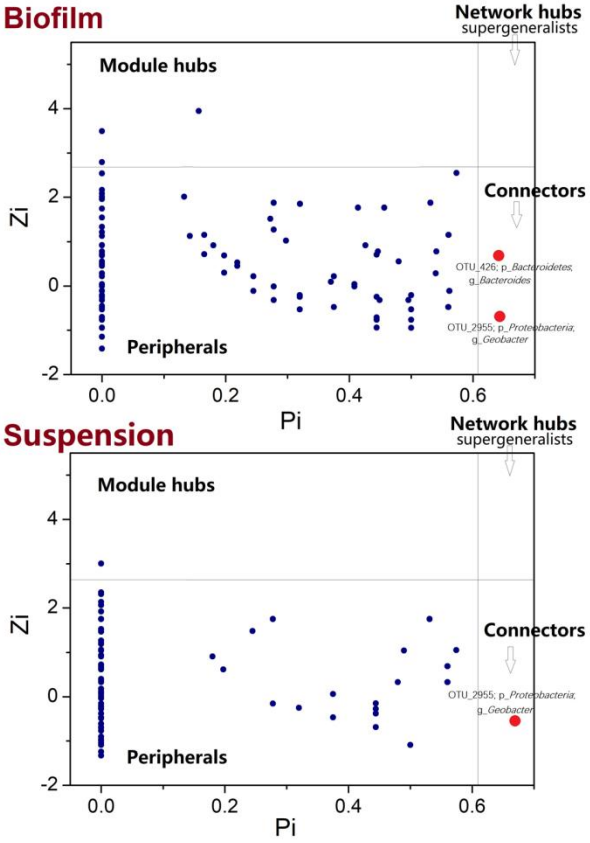

Figure S10. Results of statistical analysis illustrating similarity of bacterial communities from BPS acclimated biofilm and suspension.

(A) principal coordinates analysis (PCoA) (with the sample for their corresponding ^{13}C heavy fraction);

(B) partial least squares discriminant analysis (PLS-DA) for clustering bacteria communities from BPS acclimated biofilm and suspension;

(C) loading plot of top 15 contributors to differences in the bacteria communities between biofilm and suspension that were identified using partial least-squares discriminant analysis (PLS-DA). Related to Figure 4.

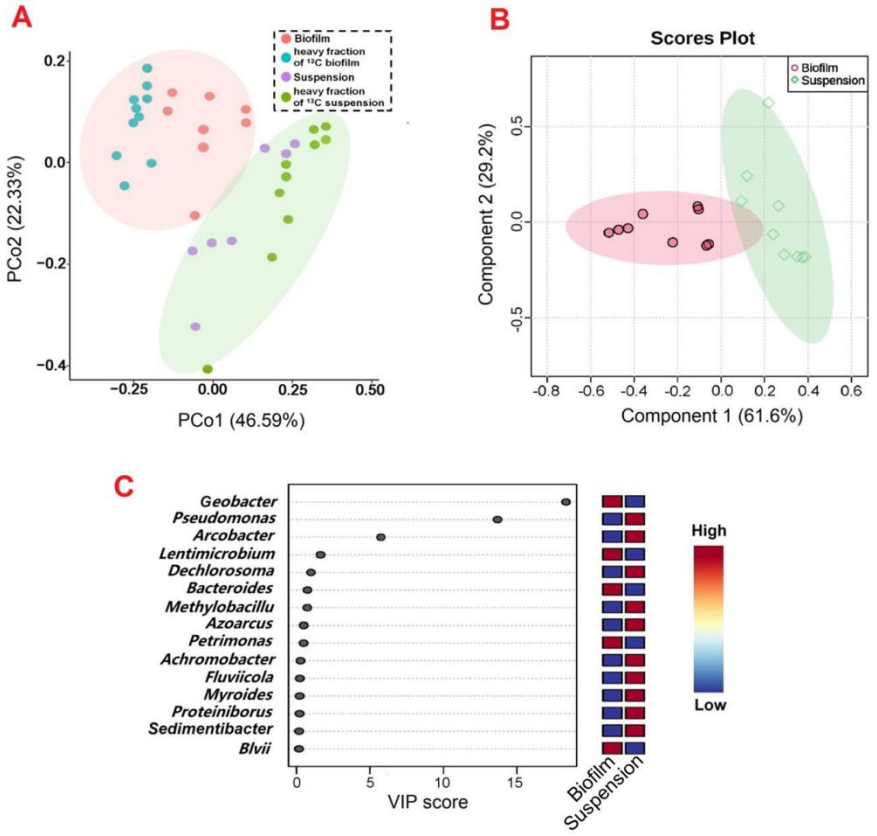

Figure S11. Cyclic voltammetry (CV) recorded of the suspending based BES.
Test conditions: a scan rate of 10 mV/s, a clean graphite without biofilm assembled as the BES anode. Related to Figure 1.

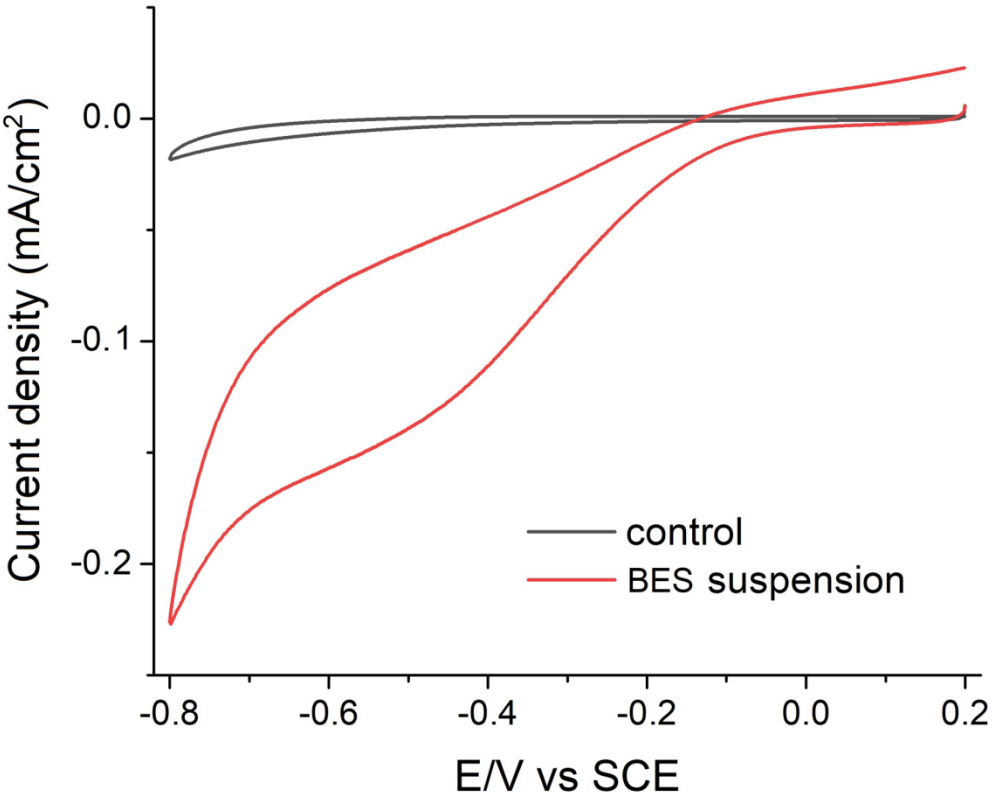

REFERENCE

Baran, R., Bowen, B.P., Bouskill, N.J., Brodie, E.L., Yannone, S.M. and Northen, T.R. (2010) Metabolite Identification in Synechococcus sp. PCC 7002 Using Untargeted Stable Isotope Assisted Metabolite Profiling. Analytical Chemistry 82(21), 9034-9042.

Bueschl, C., Kluger, B., Neumann, N.K.N., Doppler, M., Maschietto, V., Thallinger, G.G., Meng-Reiterer, J., Krska, R. and Schuhmacher, R. (2017) MetExtract II: A Software Suite for Stable Isotope-Assisted Untargeted Metabolomics. Analytical Chemistry 89(17), 9518-9526.

Cao, B., Ahmed, B., Kennedy, D.W., Wang, Z., Shi, L., Marshall, M.J., Fredrickson, J.K., Isern, N.G., Majors, P.D. and Beyenal, H. (2011) Contribution of Extracellular Polymeric Substances from Shewanella sp. HRCR-1 Biofilms to U(VI) Immobilization. Environmental Science & Technology 45(13), 5483-5490.

Deng, Y., Jiang, Y.H., Yang, Y., He, Z., Luo, F. and Zhou, J. (2012) Molecular ecological network analyses.

Doppler, M., Kluger, B., Bueschl, C., Schneider, C., Krska, R., Delcambre, S., Hiller, K., Lemmens, M. and Schuhmacher, R. (2016) Stable Isotope-Assisted Evaluation of Different Extraction Solvents for Untargeted Metabolomics of Plants. International journal of molecular sciences 17(7), 1017.

Fernando, I., Lu, D. and Zhou, Y. (2020) Interactive influence of extracellular polymeric substances (EPS) and electrolytes on the colloidal stability of silver nanoparticles. Environmental Science: Nano.

Li, J., Luo, C., Song, M., Dai, Q., Jiang, L., Zhang, D. and Zhang, G. (2017) Biodegradation of Phenanthrene in Polycyclic Aromatic Hydrocarbon-Contaminated Wastewater Revealed by Coupling Cultivation-Dependent and -Independent Approaches. Environmental Science & Technology 51(6), 3391-3401.

Ling, N., Zhu, C., Xue, C., Chen, H., Duan, Y., Peng, C., Guo, S. and Shen, Q. (2016) Insight into how organic amendments can shape the soil microbiome in long-term field experiments as revealed by network analysis. Soil Biology and Biochemistry 99, 137-149.

Song, M., Jiang, L., Zhang, D., Luo, C., Wang, Y., Yu, Z., Yin, H. and Zhang, G. (2016) Bacteria capable of degrading anthracene, phenanthrene, and fluoranthene as revealed by DNA based stable-isotope probing in a forest soil. Journal of Hazardous Materials 308, 50-57.

Sun, X., Wang, J., Li, Y., Jin, J., Zhang, B., Shah, S.M., Wang, X. and Chen, J. (2014) Highly selective dummy molecularly imprinted polymer as a solid-phase extraction sorbent for five bisphenols in tap and river water. Journal of Chromatography A 1343, 33-41.

Wagner, M., Ivleva, N.P., Haisch, C., Niessner, R. and Horn, H. (2009) Combined use of confocal laser scanning microscopy (CLSM) and Raman microscopy (RM): Investigations on EPS – Matrix. Water Research 43(1), 63-76.

Yan, W., Sun, F., Liu, J. and Zhou, Y. (2018) Enhanced anaerobic phenol degradation by conductive materials via EPS and microbial community alteration. Chemical Engineering Journal 352, 1-9.

Yang, T., Wang, L., Liu, Y., Huang, Z., He, H., Wang, X., Jiang, J., Gao, D. and Ma, J. (2019) Comparative study on ferrate oxidation of BPS and BPAF: Kinetics, reaction mechanism, and the improvement on their biodegradability. Water Research 148, 115-125.

Yuan, B.-F., Zhu, Q.-F., Guo, N., Zheng, S.-J., Wang, Y.-L., Wang, J., Xu, J., Liu, S.-J., He, K., Hu, T., Zheng, Y.-W., Xu, F.-Q. and Feng, Y.-Q. (2018) Comprehensive Profiling of Fecal Metabolome of

Mice by Integrated Chemical Isotope Labeling-Mass Spectrometry Analysis. Analytical Chemistry 90(5), 3512-3520.
Yuan, Y., Zhou, S., Xu, N. and Zhuang, L. (2011) Microorganism-immobilized carbon nanoparticle anode for microbial fuel cells based on direct electron transfer. Applied Microbiology and Biotechnology 89(5), 1629-1635.
Zhan, Y., Liu, W., Bao, Y., Zhang, J., Petropoulos, E., Li, Z., Lin, X. and Feng, Y. (2018) Fertilization shapes a well-organized community of bacterial decomposers for accelerated paddy straw degradation. Scientific Reports 8(1), 7981.